THE EFFECT OF PRIMARY SILICON REFINEMENT ON THE MICROSTRUCTURE AND PROPERTIES OF HYPEREUTECTIC ALUMINUM-SILICON ALLOYS

by

GEORGE CLAUDE WOOTTON

A THESIS SUBMITTED IN PARTIAL FULFILLMENT
OF THE REQUIREMENTS FOR THE DEGREE OF
MASTER OF APPLIED SCIENCE
IN THE DEPARTMENT
OF
MINING AND METALLURGY

We accept this thesis as conforming to the
standard required from candidates for
the degree of MASTER OF APPLIED SCIENCE

Members of the Department of Mining and Metallurgy

THE UNIVERSITY OF BRITISH COLUMBIA

February, 1959

ABSTRACT

The effect on microstructure and strength properties of hypereutectic aluminum - 20% silicon alloys of various refining additions has been studied by means of metallographic observations, hardness tests and a quantitative determination of the interparticle spacing for the primary silicon. A mechanism has been proposed to explain the observed coarsening of the eutectic which accompanies primary silicon refinement, and the combined effect of the improvement of primary dispersion and increased eutectic coarseness on strength properties has been discussed. Refining mechanisms for the refining additions used have been suggested and the reasons for the observed effect of the various refining additions on the shape of primary silicon have been presented. An explanation is offered for the increase in primary refinement which results from an increase in the time the alloy is held molten after fluxing with phosphorus pentachloride. The apparently anomalous behavior of phosphorus-copper refined alloys has been explained on the basis of the degree of dissemination of the phosphorus in the molten alloy.

Feb 16, 1959

Feb. 16, 1959

In presenting this thesis in partial fulfilment of the requirements for an advanced degree at the University of British Columbia, I agree that the Library shall make it freely available for reference and study. I further agree that permission for extensive copying of this thesis for scholarly purposes may be granted by the Head of my Department or by his representatives. It is understood that copying or publication of this thesis for financial gain shall not be allowed without my written permission.

Department of Mining and Metallurgy

The University of British Columbia,
Vancouver 8, Canada.

Date February 16th, 1959.

ACKNOWLEDGEMENT

The author is grateful for financial aid in the form of a research assistantship provided by the National Research Council and the Defence Research Board of Canada under Research Grant 7510-32.

The author gratefully acknowledges the assistance of Dr. J. A. Lund, the director of this research.

Special thanks are extended to Mr. R. G. Butters for technical advice and Mr. R. Richter for assistance with equipment.

TABLE OF CONTENTS

TABLE OF CONTENTS (cont'd.)

LIST OF FIGURES

LIST OF FIGURES (cont'd.)

LIST OF TABLES

THE EFFECT OF PRIMARY SILICON REFINEMENT ON THE MICROSTRUCTURE AND PROPERTIES OF HYPEREUTECTIC ALUMINUM-SILICON ALLOYS

I. INTRODUCTION

The use of hypereutectic aluminum-silicon alloys containing 18 to 22% silicon was suggested by a need for lighter, stronger, and more wear-resistant piston alloys than the eutectic aluminum - 11.6% silicon alloys used previously.

One of the problems first encountered in the foundry with the hypereutectic alloys was coarse primary crystallization. Primary silicon crystals are less dense than the surrounding melt and, when coarse, tend to segregate to the upper surface of a casting. Further, the primary contributes little to the mechanical properties of the alloy unless it is finely distributed.

The observation was first made in Austria that certain phosphorus-bearing substances, when added to the liquid hypereutectic alloys prior to casting, caused substantial refinement of primary silicon. The refining mechanism was not understood at the time.

A. Mechanisms of Grain Refinement.

A discussion of possible grain-refining mechanisms will be necessary before proceeding with a description of the recent work done specifically with aluminum-silicon alloys.

Grain refinement of cast alloys can be attributed in general to:

1. the restriction of the growth of crystallites by their surroundings.

2. increased rate of nucleation of the crystallite.

1. Growth-restriction.

Any mechanism which retards crystal growth will induce undercooling and nucleation of new crystals elsewhere in the liquid matrix and so will cause refinement of the resulting solid.

The retardation of crystal growth can occur as a consequence of concentration gradients, adsorption effects, and viscosity effects.

Concentration gradients arise when the inherent rate of crystal growth exceeds the rate of diffusion of atoms of the desired species to the growing crystallites.

Cibula[1] found that concentration gradients induced by the addition of various alloying elements to pure aluminum caused substantial grain refinement of aluminum. He observed that the degree of refinement increased with increasing solute concentration. Northcott[2] found with copper alloys that the concentration-gradient effect increased with an increase of the freezing range of the alloy. Cibula reported that the freezing range did not appear to be a factor directly controlling grain size but that the absolute composition interval between the liquid and co-existing solid, the slope of the liquidus curve, and to a lesser extent the slope of the solidus curve were important. This was based on a study of aluminum-copper and aluminum-nickel alloys.

The effect of adsorption of foreign atoms on the surface of crystallites of pure copper during solidification has been reported by

Northcott.[3] He studied the effect of very small additions (0.1% to 2%) of approximately 35 elements to pure copper on the reduction of the tendency towards columnar growth and found that some of the elements were more effective than others. This difference was explained as a difference in the tenacity of the adsorbed layer of impurity atoms on the copper crystals. His explanation of refinement on the basis of an adsorption model was substantiated by the fact that, in several cases, he found no increase in refinement over a wide range of solute concentrations above a certain low minimum value.

The growth-restricting effect of high viscosity of the liquid medium surrounding a growing crystal has not been definitely established experimentally. However, Smithells[4] suggests that viscosity might have had some effect on the growth-restriction noted by Northcott.

2. Rate of nucleation.

An increase in the rate of nucleation can be brought about either by increasing the rate of cooling or by introducing artificial nuclei to the molten material. This is best illustrated diagrammatically using the method of Becker, described by Mehl and Jetter.[5] The total free energy change involved in the formation of a crystallite, $\triangle G'$ in Figure 1 is the sum of two terms

$$\triangle G' = \triangle G_1' + \triangle G_2'$$

where $\triangle G_2'$ is the work of formation of the crystallite-liquid interface, which is positive and is proportional to the square of the linear dimensions of the crystallite; and $\triangle G_1'$ is the negative free energy change resulting from a phase change at a given degree of undercooling , and which is proportional to the cube of the crystallite diameter.

If $\triangle G'$ in Figure 1 is taken as the total free energy change in the formation of a crystallite at a certain degree of undercooling, then at a

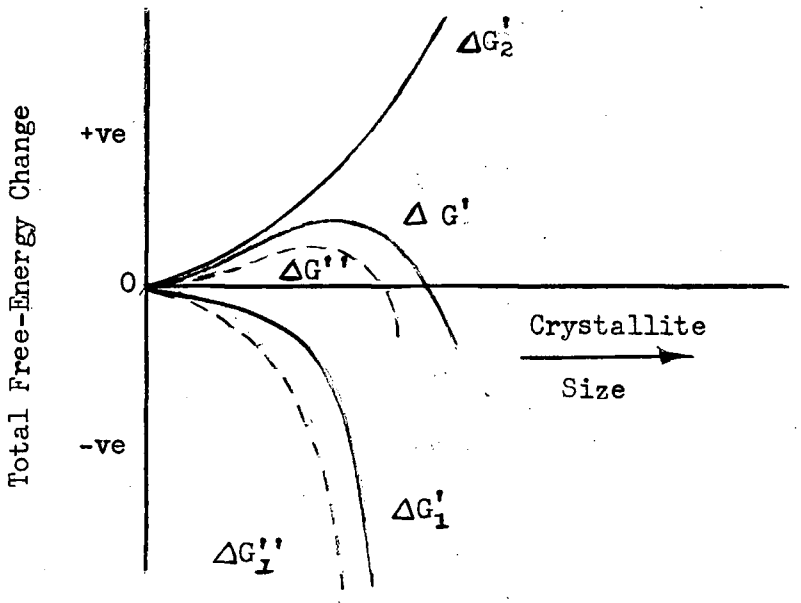

Figure 1. Effect of undercooling on free energy of formation of crystallite.

larger degree of undercooling $\triangle G''$ will represent the total free energy change. The suppression of the maximum in $\triangle G''$ is caused by the increase in the negative free energy change resulting from the phase change, $\triangle G_1''$, as shown in Figure 1. If all other things remain constant, an increase in cooling rate will cause an increase in undercooling, and therefore an increase in the cooling rate will increase the rate of nucleation by decreasing the total free energy change required for the formation of nuclei.

In the case of artificial nuclei the total free-energy change for a certain degree of undercooling corresponding to $\triangle G'$ will be decreased to $\triangle G'''$, Figure 2, by the corresponding decrease in $\triangle G_2'$, the work of formation of the crystallite liquid interface. Only certain foreign particles have the ability to reduce the work of formation of the crystallite liquid interface. This is discussed more fully in Appendix A.

The work of Turnbull[6,7] has shown that the presence of solid

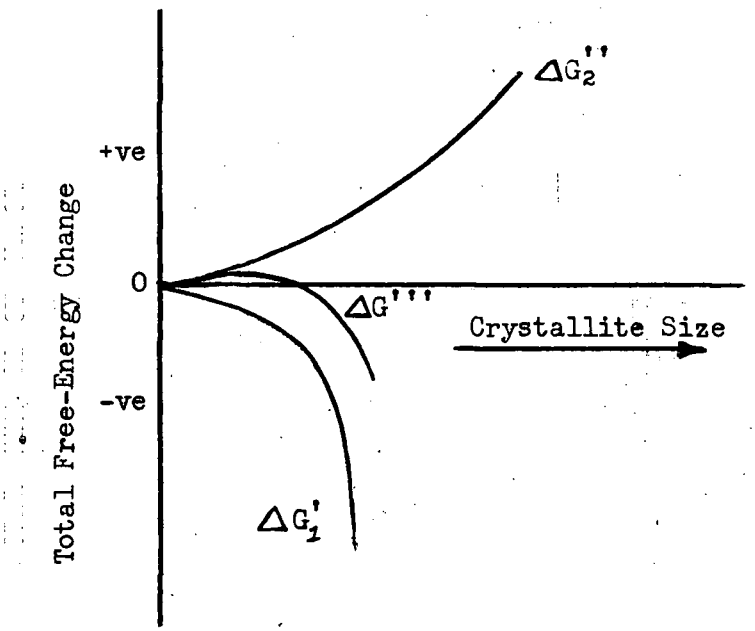

Figure 2. Effect of foreign nuclei on free energy of formation of crystallite.

heterogeneities in a liquid metal may greatly reduce the undercooling observed prior to the commencement of solidification.

There are a number of possible sources of solid heterogeneities in liquid metals, including:

a. accidental inclusions such as oxide, etc.

b. fragments of solidified metal dendrites broken off by turbulence during casting and injected into a molten region of the casting.

c. intermetallic compounds of the alloying materials or compounds of the alloying materials and impurities, which may form in the liquid alloy and which are stable at the casting temperature.

d. particles of the solid alloy added intentionally or present in crevices in the mould walls.

The effect of non-metallic inclusions on the grain-size of cast iron, steel, and aluminum was studied by Mitsche.[8] He observed that the grain-size was either refined or coarsened depending upon the size and concentration of the inclusions in the liquid metal.

The equiaxing observed in some brasses has been attributed to erosion and injection of solid particles into the liquid from the solidified skin by pouring turbulence. Mitsche[8] and Latin[9] reported refinement by this mechanism.

Several mechanisms have been postulated for the observed refining effect of titanium and other transition metals on pure aluminum. The most recent, and probably the most valid proposal has been made by Cibula[1,10] who concluded that the transition metals react with residual carbon in the melt to form simple carbides which are solid at the casting temperature and which nucleate solidification on cooling. In the case of titanium, Cibula verified the presence of titanium carbide by X-ray diffraction. He also proposes that the refinement of aluminum and aluminum alloys by boron is due to the nucleation of solidification by the intermetallic compound AlB_2.

Based on his work, Cibula[1] has advanced the following comprehensive mechanism for grain-refinement of cast aluminum solid-solution alloys:

a) the restriction of grain growth by concentration gradients causes undercooling at the surface and into the interior of a casting which produces an equi-axial structure. Grain-refinement by this mechanism is rarely very marked.

b) the presence of nuclei upon which the aluminum solid solution can crystallize readily is associated with almost complete suppression

of undercooling. This mechanism alone will refine a coarse columnar structure to a fine columnar structure.

c) the combination of concentration gradients and active nuclei gives marked grain-refinement associated with little, if any, undercooling. This mechanism will refine coarse columnar grains to fine equi-axial grains.

B. Refinement of Hypereutectic Aluminum-Silicon Alloys.

Onitsch-Modl[11] studied qualitatively the effect of various refining additions on the structure of hypereutectic aluminum-silicon (18 to 22% silicon) piston alloys. She reported that a desirable structure was obtained when a mixture of ground aluminum - 12% silicon alloy, pure aluminum chips, and sodium was added to the molten alloy immediately prior to casting. Other additions (metallic titanium, an aluminum-titanium compound, phosphorus pentachloride, and a phosphorus copper alloy) caused substantial refinement of primary crystallization but did not affect the eutectic structure. Two refinement mechanisms were suggested by Onitsch-Modl.

1. Finely divided metallic agents increase the number of artificial nuclei already present in the melt and thereby induce fine primary solidification.

2. Other additives appear to destroy or inactivate nuclei present in the melt and cause extended undercooling and fine-grained solidification due to homogeneous nucleation.

It was shown in later work by Lund[12] that the second of these two proposed mechanisms was incorrect and that in the case of phosphorus additions, primary refinement was caused by the nucleation of silicon by

aluminum phosphide (AlP) particles which formed in the molten alloy. Lund also reported refinement by arsenic and attributed this to the formation of dispersed aluminum arsenide (AlAs) in the molten alloy. Both AlP and AlAs are stable well above the casting temperature and both have lattices and crystal structures similar to that of silicon (see Table 1).

TABLE 1

Crystallographic Data for Silicon, Aluminum Phosphide and Aluminum Arsenide.

	Lattice Parameter Å	Crystal Structure	Reference
Silicon	5.4198	Diamond Cubic	13
Aluminum Phosphide	5.42	Zinc Blende	13
Aluminum Arsenide	5.62	Zinc Blende	13

The chemical form of the phosphorus addition was found to be important to the degree of refinement afforded, phosphorus pentachloride being more effective than elemental phosphorus or phosphorus copper. This was explained by the fluxing effect of the pentachloride, which would contribute to the removal of impurity atoms that might otherwise prevent phosphide formation or inactivate the aluminum phosphide particles by reaction or adsorption.

It was also observed that magnesium causes limited refinement of primary silicon but that phosphorus plus magnesium causes much greater refinement than either addition alone. The effect of magnesium alone was explained by the restriction of crystal growth due to adsorption of magnesium onto the primary silicon, while the combined effect was thought to be the result of nucleation of primary silicon and then restriction of its growth by adsorption. This would force nucleation of silicon to occur on new aluminum phosphide

particles.

Lund proposes, on the basis of the above work and work reported in the literature, a modified theory of nucleation of the primary phase in a binary alloy. He considers the combined effects of heterogeneous nucleation of the primary phase by particles of varying activities (see Appendix A) and concentration gradients around the primary phase, caused by the alloying element, on the degree of primary refinement afforded by a particular addition.

Mascré[14] reported the results of a study of the effect of additions of sodium, phosphorus-copper, and sodium plus phosphorus-copper on both the mechanical properties and microstructure of an aluminum - 20% silicon - 1.8% copper alloy. In the case of sodium additions alone he observed that with a small amount of sodium (0.05%) the eutectic had a modified form and was very fine, while the primary was relatively coarse and dendritic. With a larger amount of sodium (1%) the eutectic was still very fine but the primary silicon particles assumed a spherical shape.

The variation in rupture strength with sodium content observed by Mascré is shown in Figure 3. It is interesting to note that sodium

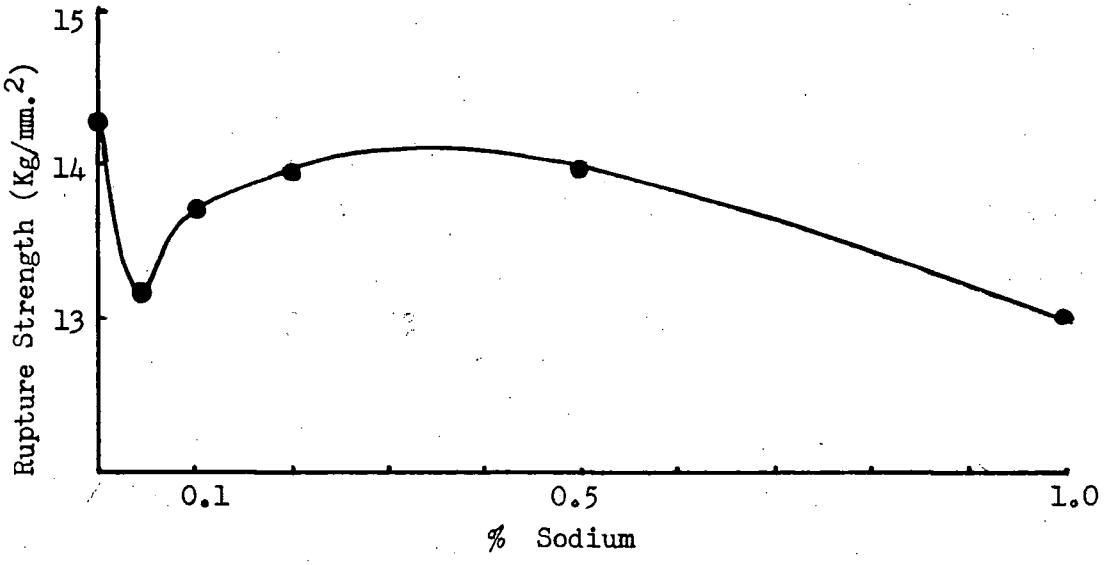

Figure 3. Variation in rupture strength with sodium content for aluminum-silicon-copper alloy.[14]

modification caused a decrease in the strength of the hypereutectic alloy contrary to the results for hypoeutectic alloys.

In the case of alloys refined by phosphorus-copper additions, Mascre reported that 0.01% phosphorus caused extreme refinement of the primary solidification and that the eutectic was unmodified and very coarse. Larger amounts of phosphorus did not contribute to the further refinement of primary silicon but did refine the eutectic which reportedly had an extremely fine modified structure at the 0.025% phosphorus level.

The variation of mechanical properties with phosphorus content reported by Mascre is shown in Figure 4. Brinell hardness followed the rupture strength curve of Figure 4 rising from 86 for the unrefined alloy to 93 for the alloy containing 0.01% phosphorus.

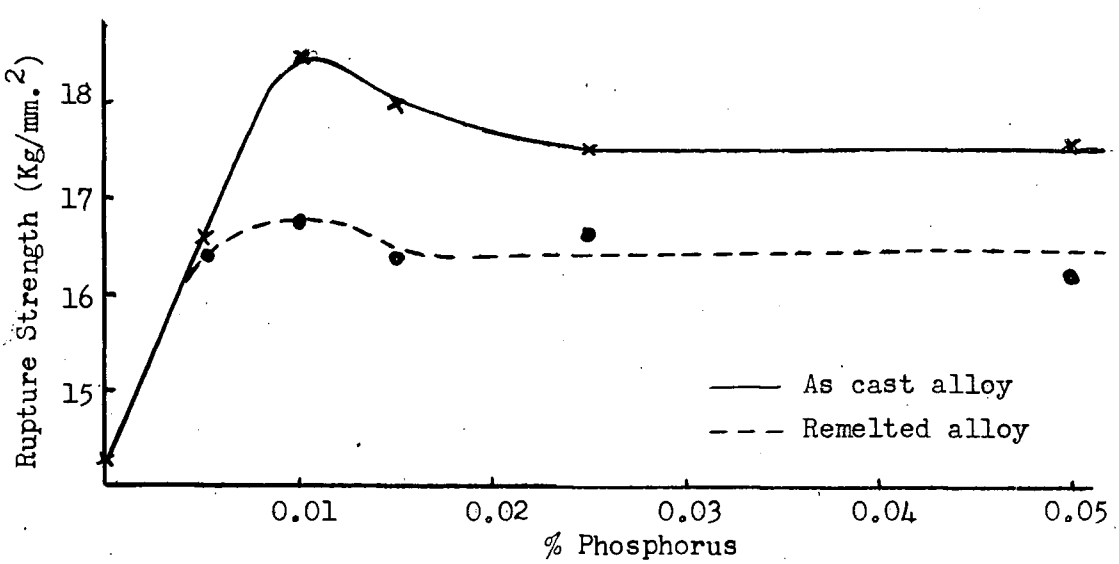

Figure 4. Variation in rupture strength with phosphorus content for aluminum-silicon-copper alloy.[14]

In Mascre's work with alloys containing sodium and phosphorus additions the phosphorus content was fixed at 0.01% and the sodium content was varied. For a small addition of sodium the primary silicon was not only dendritic but was also elongated. The eutectic was always fine with a

modified form.

Mechanical properties for alloys containing sodium and phosphorus were intermediate between those for sodium alone and those for phosphorus alone. The rupture strength of a 0.01% phosphorus refined alloy decreased with increased sodium content as shown in Figure 5.

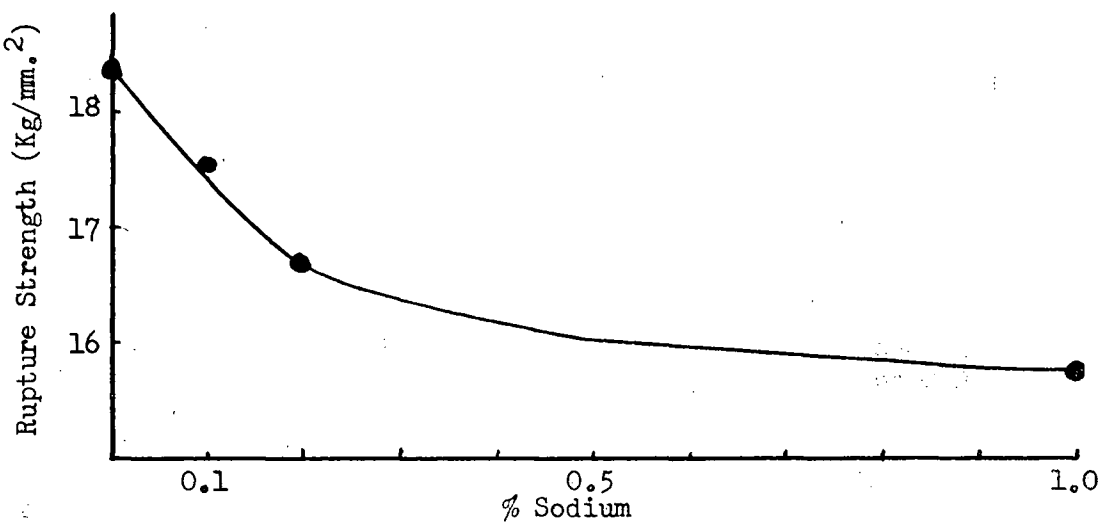

Figure 5. Variation in rupture strength with sodium content for aluminum-silicon-copper alloy refined by 0.01% phosphorus.[14]

Mascré reported that the effect of sodium was lost if the alloy was held molten for more than a few minutes after addition, and was always lost on remelting the solidified alloy. However, the effect of phosphorus lasted even when the alloy was held molten for an hour after a phosphorus-copper addition and was only partially lost on remelting as shown in Figure 4.

Mascre explained the variation in the shape of primary silicon due to sodium additions on the basis of a concentration gradient effect. He offered no explanation for the variation in mechanical properties with different additions, for the variation in eutectic refinement with various additions, or for the change in shape of primary silicon with phosphorus

additions.

It has been noted in the works previously cited that the aluminum-silicon eutectic has varied between a coarse normal form and a fine 'modified' form. Chalmers[15] has reported that a modified eutectic can be obtained in aluminum-silicon alloys either by rapid cooling or by the addition of small amounts of sodium. The mechanism of refinement by rapid cooling is discussed in a later section. The theory proposed by Chalmers to explain sodium modification is based on the effect of sodium on the interfacial angles between solid aluminum, solid silicon, and the liquid during solidification of the eutectic. It is postulated that sodium decreases the surface energy of the aluminum-silicon solid interface, thereby increasing angle Θ in Figure 6a to that shown in Figure 6b. This gives the aluminum a lead in growth over the silicon as shown and since growth is at right angles to the growing surface, the aluminum quickly surrounds the silicon, sealing it off (Figure 6c) and forcing the nucleation of new silicon. This gives rise to a fine or 'modified' eutectic structure.

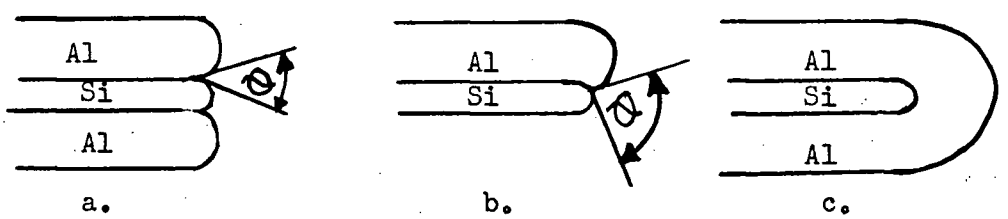

Figure 6. Effect of sodium on aluminum-silicon eutectic solidification.[15]

C. Studies of Dispersion Hardening.

The first work which suggested that there might be a correlation between the mechanical properties of an alloy and its microstructure was due to Sorby[16] in 1887. His work has since been extended until today correlations

between microstructure and properties are widely used industrially.

Greene[17] found a definite relationship between the interlamellar spacing and Brinell hardness number of pearlite and between the interlamellar spacing and ultimate strength of pearlite in eutectoid rail steels.

Gensamer, Pearsall, and Smith[18] obtained a straight line relationship between interlamellar spacing and strength properties for plain carbon eutectoid steels.

Gensamer, Pearsall, Pellini, and Low[19] have proposed a rule of strength for the case of a hard phase dispersed in a softer phase, on the basis of their work with plain carbon eutectoid steel. Their rule is that 'the resistance to deformation of a metallic aggregate consisting of a hard phase distributed in a softer one is proportional to the logarithm of the mean straight path through the continuous phase'.

Shaw, Shepard, Starr, and Dorn,[20] found that the plastic properties of two phase aluminum-copper alloys correlated with the mean free path between hard $CuAl_2$ particles dispersed in the alpha solid solution.

Roberts, Carruthers and Averbach[21] extended the work on eutectoid steels to those having a mixed microstructure. They found that the elastic limit and lower yield point are linear functions of the logarithm of the mean ferrite path (Figure 7), if this parameter is defined as follows:

Structure	Mean Ferrite Path
Spheroidite	Mean distance between carbide particles along a straight line.
Ferrite- pearlite	Mean distance from one pearlite patch to the next or to a ferrite grain boundary as intercepted along a straight line.
Ferrite	Mean distance between inclusions and grain boundaries along a straight line.

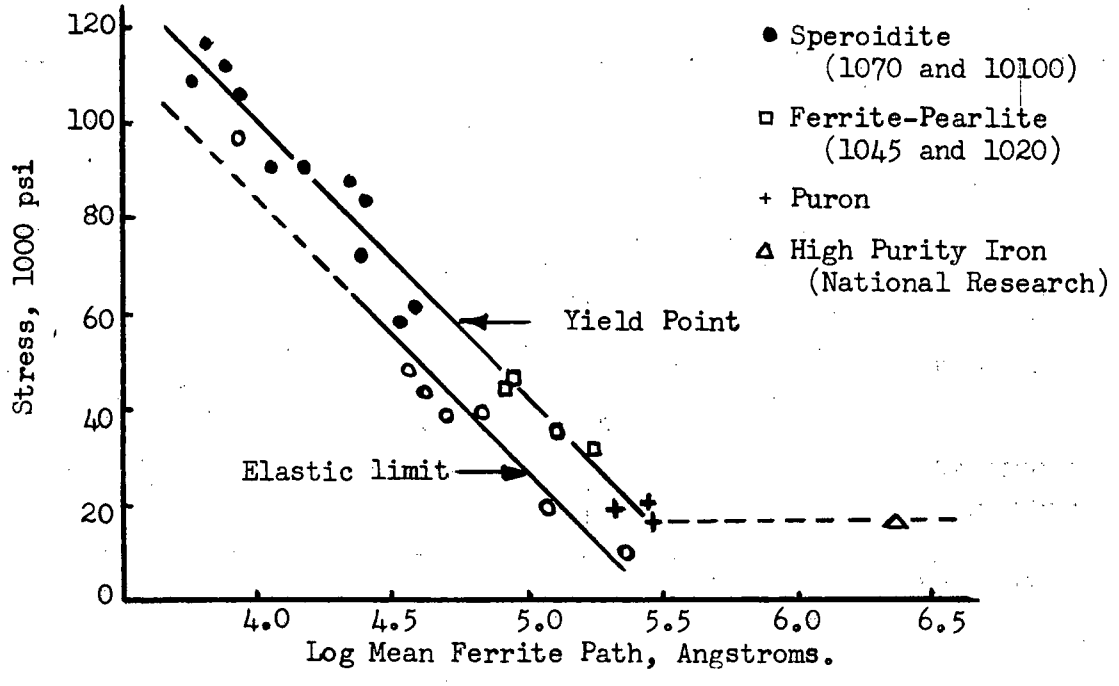

Figure 7. Variation in yield point and elastic limit with fineness of the microstructure.[21]

In an attempt to explain the effectiveness of a dispersed hard phase on the hardening of metals, theories of dispersion hardening have been postulated by Mott and Nabarro,[22] Orowan,[23] and Fisher, Hart and Pry.[24] These are presented and appraised in a paper by Hart.[25]

These theories all explain the increase in strength with decreasing mean free path between the hard phase particles on the basis of the restricting effect exerted by the hard particles on the motion of dislocations.

On the basis of the foregoing it might be expected that, providing the eutectic structure was not altered, an improvement in mechanical properties should accompany a refinement of the primary silicon phase in hypereutectic aluminum-silicon alloys.

Although the mechanism for the refinement of primary silicon by phosphorus is now understood there remain a number of unexplained results.

These are:

1. the effects of primary refining additions on the structure of the eutectic.
2. the effect of additives other than phosphorus on primary and eutectic solidification.
3. the effect of the time the alloy is held molten after refining additions are made.
4. the reason for the observed effect of the sequence of addition of refiners, when more than one is used in the same alloy.
5. the observed change in the shape of primary silicon with refining additions.
6. the reason for the apparent existence of an optimum phosphorus content in the case of phosphorus-copper additions.

The purpose of the present work is to explain, where possible, the above observations and to attempt to determine quantitatively the importance of primary particle size on the mechanical properties of an aluminum - 20% silicon alloy.

II. EXPERIMENTAL

A. Preparation of Master Alloys.

Two aluminum - 20% silicon master alloys were prepared by induction melting pure aluminum* in fire-clay crucibles, which had been lined with Norton Company RA1162 Alundum Cement and fired at 1000°C, and adding pure silicon to the melts. The melts were thoroughly stirred and cast from 800°C into chalked steel button-moulds. No loss of aluminum or silicon was observed in melting and there was no reason to expect any segregation of the components. A total of 22 buttons weighing approximately 100 grams each was obtained.

B. Preparation and Casting of Experimental Alloy Melts.

It was originally planned to carry out all melting, alloying, and casting operations in purified argon. A controlled-atmosphere high-frequency induction melting and casting unit was constructed for this purpose prior to the commencement of experimental work. A number of factors, however, made the use of this unit unattractive. In the first place, temperature control in the high frequency furnace at the several temperature levels required was unsatisfactory. Also, the phosphorus pentachloride additions used in the present work had to be added after melting and alloying, and the additions resulted in the liberation of copious quantities of chlorine. These factors made the use of any totally-enclosed system impracticable. In addition, it was desired to be able to cast into moulds at different temperatures, and to be able to ensure a constant rate of pouring, both of which would have been difficult in a closed unit.

---

* For analysis of all components of alloys, see Appendix B.

It was therefore decided to work with the open system shown in Figure 8, using a chromel A-wound resistance pot furnace.

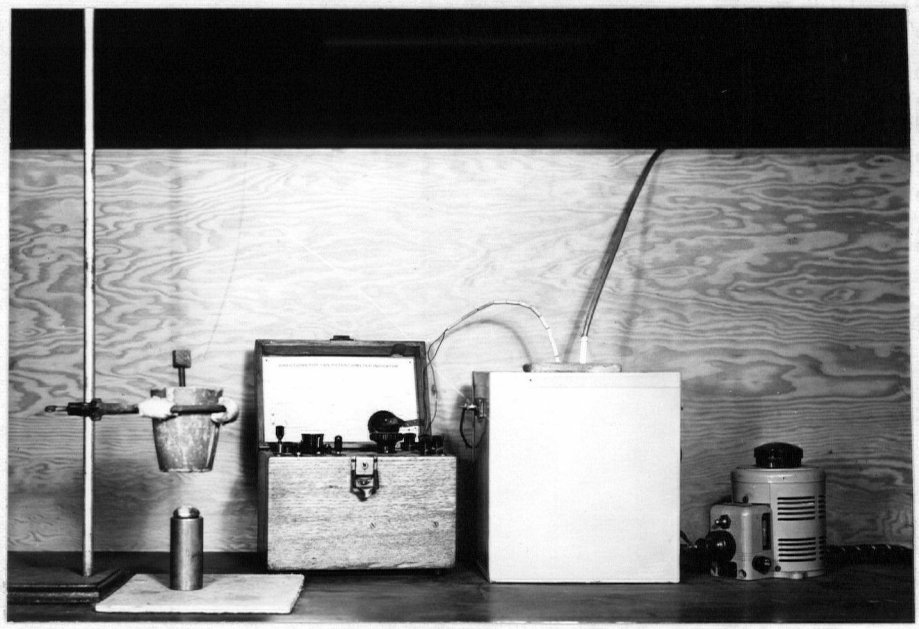

Figure 8. Melting and casting equipment.

All melts were made in fire-clay crucibles lined with Norton Company RA1162 Alundum cement and fired at 1000°C prior to use. The majority of the melts consisted of one button of master alloy weighing approximately 100 grams plus any alloying additions required. To protect the surface of these small melts from severe oxidation, the upper part of the melting crucible was flushed continuously with a flow of argon.

A calibrated 18 gauge chromel-alumel thermocouple was used in conjunction with a Leeds and Northrup potentiometer of 200 microvolt sensitivity, for temperature determinations.

Alloying elements were added to the small master-alloy melts by wrapping the additions in aluminum foil and submerging them in the molten metal. Melts were heated to 960°C before adding germanium, whereas copper and magnesium

were added at 750°C. The melts were held at temperature for five minutes to allow complete solution of the additions before any of the melts were fluxed.

Fluxing of the melts, to remove entrained gases and inclusions, was performed at 750°C. Porous carbon rods, saturated with carbon tetrachloride, were immersed in the melts and the liberated chlorine provided the fluxing action.

Phosphorus was added to the fluxed melts at 750°C either as phosphorus pentachloride or in the form of a phosphorus-copper alloy. The additions were wrapped in aluminum foil and submerged in the melts.

After refining with phosphorus the melts were transferred to a pre-heated (850°C) clay-graphite holding pot, lined with Norton RA1162 Alundum cement and fired at 1000°C. This pot had a small hole in the bottom, initially plugged with a removable carbon rod, which permitted bottom-pouring of the melt and which provided a constant rate of pouring.

All melts were cast from 710°C into copper moulds of the design shown in Figure 9. The moulds were initially at room temperature in all cases.

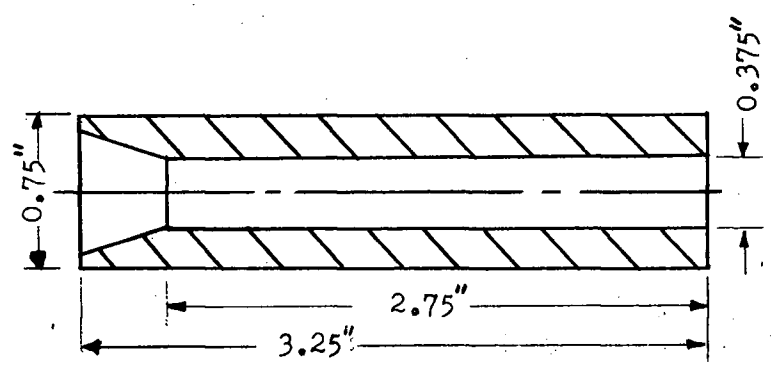

Figure 9. Section through copper mould.

C. Preparation and Testing of Specimens.

1. Tensile tests.

Tensile test bars were machined from the centre of as-cast bars to the dimensions shown in Figure 10.

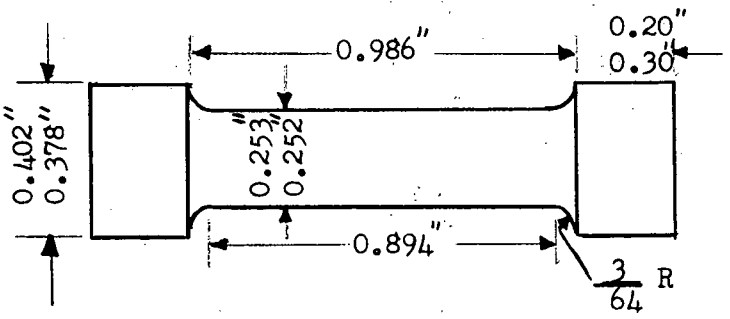

Figure 10. Dimensions of test bar.

The tensile bars were tested to fracture on a Hounsfield Tensometer.

2. Macro hardness tests.

For alloys numbered 1 to 5 and 9 to 14, specimens for macro hardness tests were prepared by mounting sections cut from the as-cast bars at locations directly above and directly below the location of the tensile specimens (see Figure 11). For the other alloys as-cast bars were sectioned in seven places and all sections not used for microexamination were used for macro hardness test specimens.

Two to five sections of bar were placed in each mount and were polished on Numbers 2 through 000 emergy paper prior to Rockwell hardness testing.

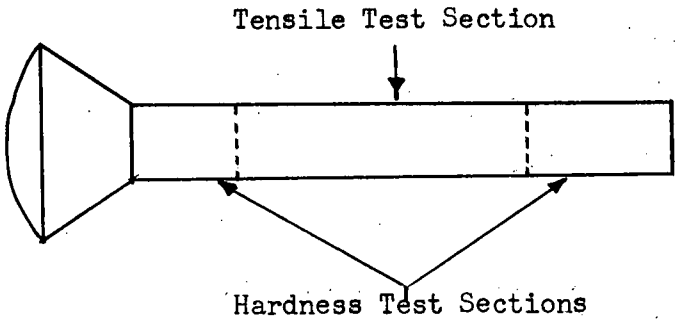

Figure 11. Location of tensile and hardness specimens in the as-cast bar.

3. Microhardness tests and microexamination.

Specimens for microexamination were obtained by mounting the undeformed ends of the fractured tensile test bars for alloys numbered 1 to 5 and 9 to 14 and the ends and centre of as-cast bars for the other alloys. Bakelite mounts were used in all cases. These specimens were polished on Numbers 2 through 000 emergy paper using kerosene as the lubricant, and then were lapped with 600 x Alundum and Linde B abrasives in turn. The etchant used was an aqueous solution of 0.5% hydrofluoric acid.

Micro hardness tests were performed on the polished and etched specimens using a Tukon Tester with a Knoop diamond indenter.

D. Dispersion Measurements.

In the following text the term 'dispersion' will refer to the dispersion of primary silicon in the aluminum-silicon eutectic matrix of the 20% silicon alloy.

Several methods of determining dispersion quantitatively were studied, and that due to Shaw, Shepard, Starr, and Dorn[20] was found to be the

most suitable.

The method of Shaw et al requires the determination of two values. These are N, the number of particles of the dispersed phase per unit area of polished section, and f, the ratio of the volume of the dispersed phase to the volume of the surrounding matrix. These are related to r, the radius of the dispersed particles, and R, the radius of the domain of the dispersed particle, by the following formulae;

$$N = \frac{3r}{2\pi R^3} \quad \text{and} \quad f = \frac{1}{\left(\frac{R}{r}\right)^3 - 1}$$

Of the two parameters f will be constant for a constant silicon content* while N may vary with minor alloying additions and cooling rate. The value of f is given by:

$$f = \frac{\text{volume of hypereutectic silicon}}{\text{volume of matrix}}$$

The values for volumes of hypereutectic silicon and eutectic can be obtained from the phase diagram for aluminum-silicon (Figure 12) as follows:

$$\text{weight \% primary silicon} = \frac{20 - 11.6}{100 - 11.6}(100) = 9.5\%$$

$$\text{weight \% eutectic} = \frac{100 - 20}{100 - 11.6}(100) = 90.5\%$$

The densities of silicon and eutectic at room temperature are 2.42 gr./cc[27] and 2.66 gr./cc.[28] Therefore,

$$f = \frac{\frac{9.5}{2.42}}{\frac{90.5}{2.66}} = \frac{3.92}{34.0} = 0.116$$

---

* For an estimate of the effect of a variation in silicon content on f, see Appendix C.

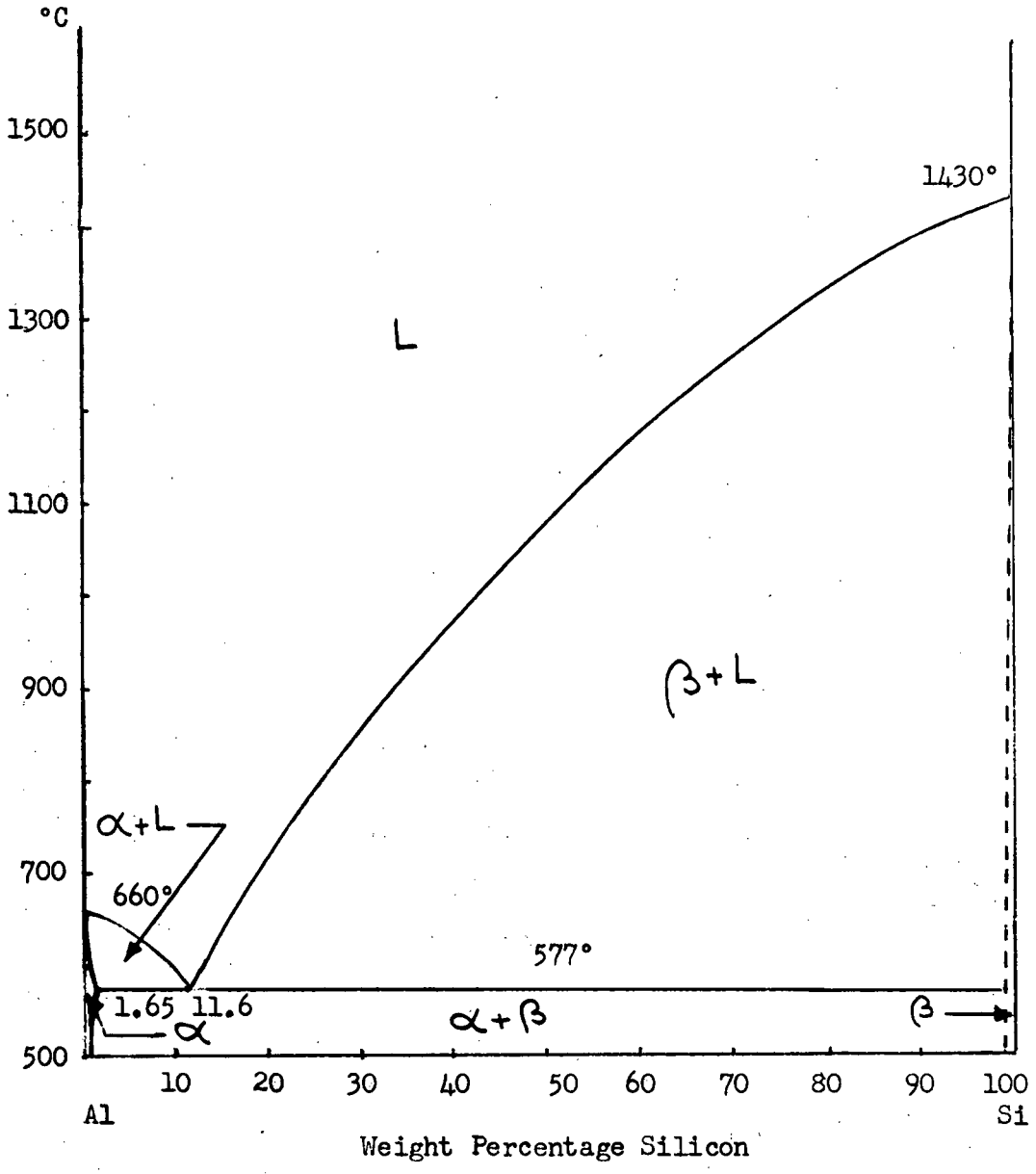

Figure 12. Aluminum-silicon phase diagram.[26]

The assumptions made in the above calculations are that the solubility of aluminum in silicon is negligible at all temperatures below the solidus[26] and that none of the silicon which is in solid solution in aluminum at the eutectic temperature (577°C) precipitates onto primary silicon particles on cooling the 20% silicon alloy to room temperature.

The latter assumption introduces the possibility of a small error in the value of f, since supersaturated α solid solution which is in the immediate proximity of the surface of primary silicon particles below 577°C will tend to precipitate some silicon onto the primary particles. Considering, however, the relative volumes occupied by the primary and eutectic constituents, and considering the high relative surface area of eutectic silicon, the amount of silicon precipitated onto primary particles would be expected to be very small compared with that which is precipitated onto eutectic silicon.

In any case, since f may be considered a constant for all alloys in the present work, an error in its absolute value will not affect the comparative values of the calculated primary dispersions.

The value of N for the various alloys was obtained by counting the number of particles of the dispersed phase in a 50 $cm.^2$ area on the ground-glass screen of a projection microscope at magnifications ranging from 100 to 325. The magnifications were chosen such that the smallest primary silicon particles present were clearly resolvable and were easily differentiated from eutectic silicon particles.

Microspecimens were traversed in two mutually perpendicular directions as shown in Figure 13. Counts were made at equal intervals along the traverse as at the crosses in Figure 13. Several specimens were traversed for each alloy.

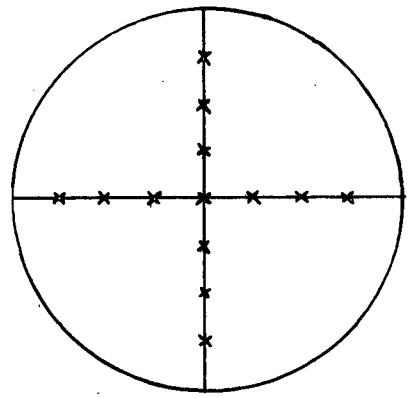

Figure 13. Location of dispersion measurements on metallographic specimen.

The value of N is obtained from

$$N = \left(\frac{\text{Average number of particles/50 cm.}^2}{50}\right)(\text{magnification})^2$$

Using the values of N obtained from the above formula and the constant value of f, for 20% silicon alloys, the values of r and R can be found for each case being studied. These in turn give a quantity described as 'volumetric mean free path' when substituted in the following equation:

$$\text{V.M.F.P.} = R\left\{\frac{1}{1 - \sqrt{1 - \left(\frac{r}{R}\right)^2}} - \frac{r}{R}\right\} = \text{P.I.S.}$$

where P.I.S. is 'primary interparticle spacing'.

In the work of Starr et al the volumetric mean free path is a measure of the distance between $CuAl_2$ particles in a homogeneous aluminum solid solution matrix. In the present work it is used as a measure of the distance between the hypereutectic silicon particles in an aluminum-silicon eutectic matrix. Since the path between primary particles is not, therefore, 'free', it is felt preferable to describe the quantity represented by the above function as 'primary interparticle spacing' in the present work.

The assumptions on which Shaw et al base their derivation of the formula for volumetric mean free path are:

(a) the dispersed particles are uniformly dispersed.

(b) the dispersed particles are spherical in shape.

Justification for the application of this formula in the present work is that any lack of uniformity of dispersion may be compensated for by using an average value of N resulting from a large number of primary particle counts across the full section of the alloy, as was done in the present work. Also, although the dispersed silicon particles have, in most cases, an angular shape, and although some error in the absolute values of primary interparticle spacing will result, the shape of the primary silicon particles is fairly uniform throughout each group of alloys. Since the spacing values are used on a comparative basis only, any error introduced by particle shape will be essentially constant and therefore not critical in the present work.

E. Statistical Treatment of Measurements.

It was felt that before complete confidence could be placed in the results of multiple hardness tests and primary interparticle spacing determinations, on the same specimen, they should be subjected to a confidence limit study. This was done for all the hardness tests and several of the primary interparticle spacings and the results presented in Table 2 show both the average value and the possible range of the average value as found by a 99% confidence limit study.

III. RESULTS AND DISCUSSION

A. Dispersion Measurements and Metallographic Observations.

The results of the metallographic observations and dispersion measurements are presented below in groups selected on the basis of alloy content.

1. Alloys containing phosphorus only

This group of alloys contained phosphorus which was added as the pentachloride salt. The compositions quoted in Tables 2 (Appendix D) and 2a are based on the weights of additions, and because of the high volatility of phosphorus pentachloride when added to molten aluminum, the true phosphorus contents of the alloys are likely to be somewhat lower than those reported. The methods for this analysis were too complex to be undertaken in the department.

The results of dispersion measurements for this group of alloys are collected in Table 2a. Alloy number 1 contained no phosphorus and is included here for comparison.

A study of Table 2a and the microstructures shown in Figures 15 to 20 reveal that:

a. primary interparticle spacings decrease with increasing phosphorus content (see Figure 14). Very little phosphorus is required to produce substantial primary refinement.

b. the average size of the primary silicon particles decreases with increasing phosphorus content (Figures 15 to 19).

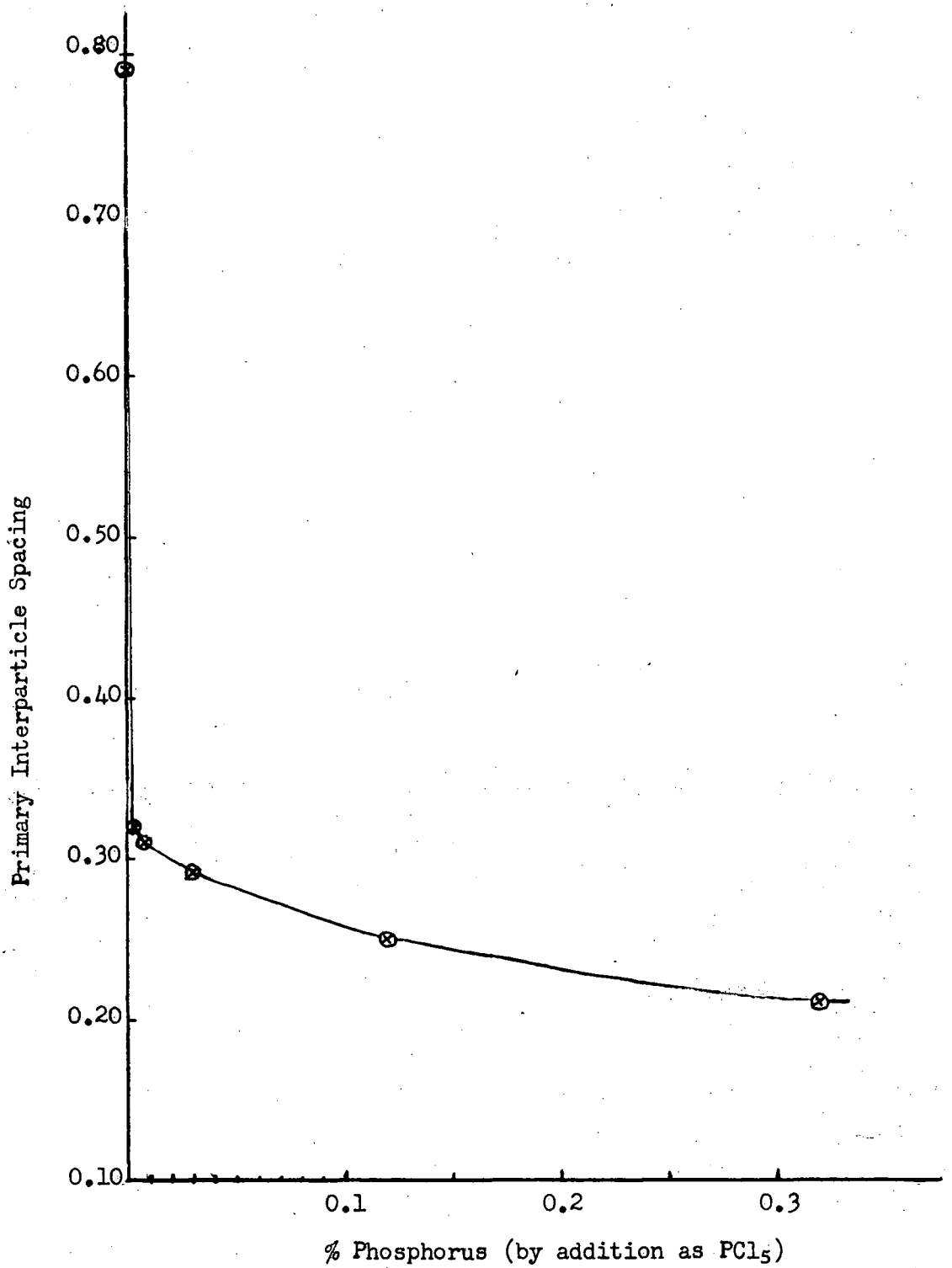

Figure 14. Variation in primary interparticle spacing with phosphorus content for phosphorus pentachloride refined alloys.

Figure 15. Alloy No. 1 unrefined.
0.5% HF etch 150X

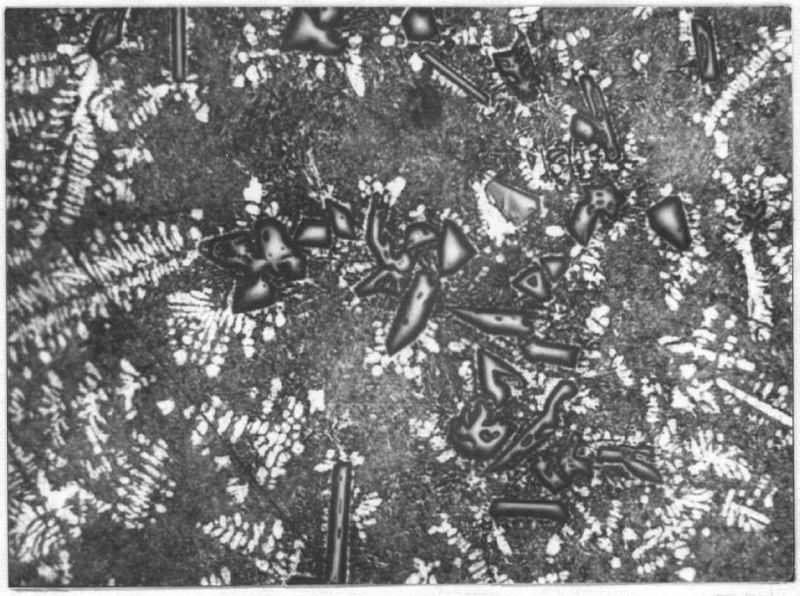

Figure 16. Alloy No.3 refined by 0.002% P added as PCl_5. Cast 5 minutes after PCl_5 added. 0.5% HF etch. 150X

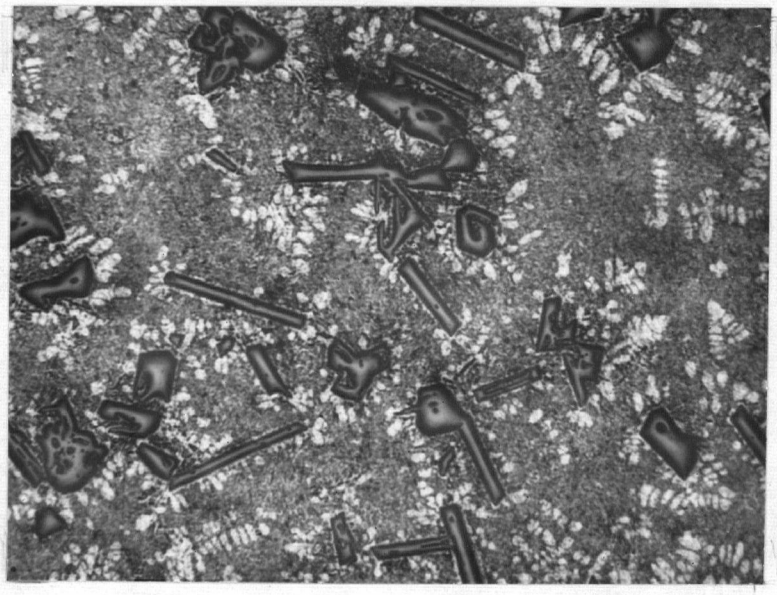

Figure 17. Alloy No.4 refined by 0.007% P added as PCl_5. Cast 5 minutes after PCl_5 added. 0.5% HF etch. 150X

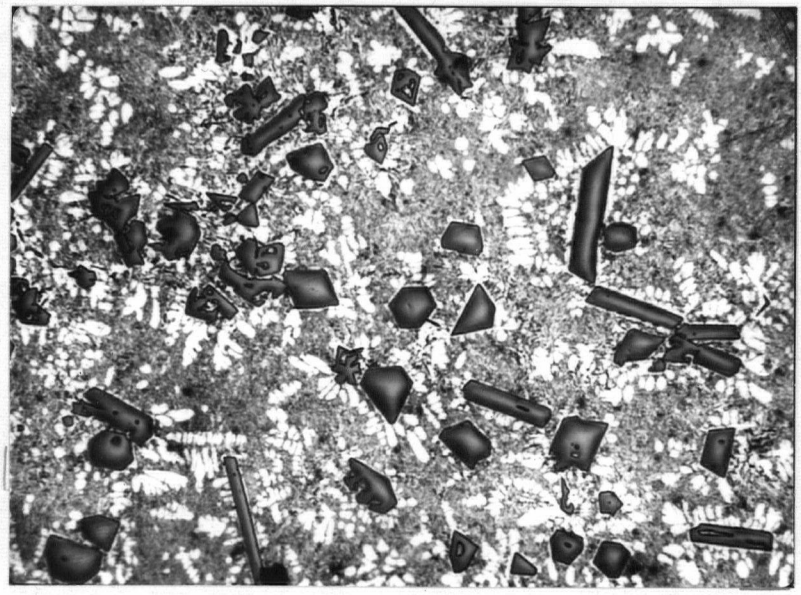

Figure 18. Alloy No.6 refined by 0.12% P added as PCl_5. Cast 5 minutes after PCl_5 added. 0.5% HF etch. 150X

Figure 19. Alloy No. 7 refined by 0.32% P added as PCl_5. Cast 5 minutes after PCl_5 added. 0.5% HF etch. 150x

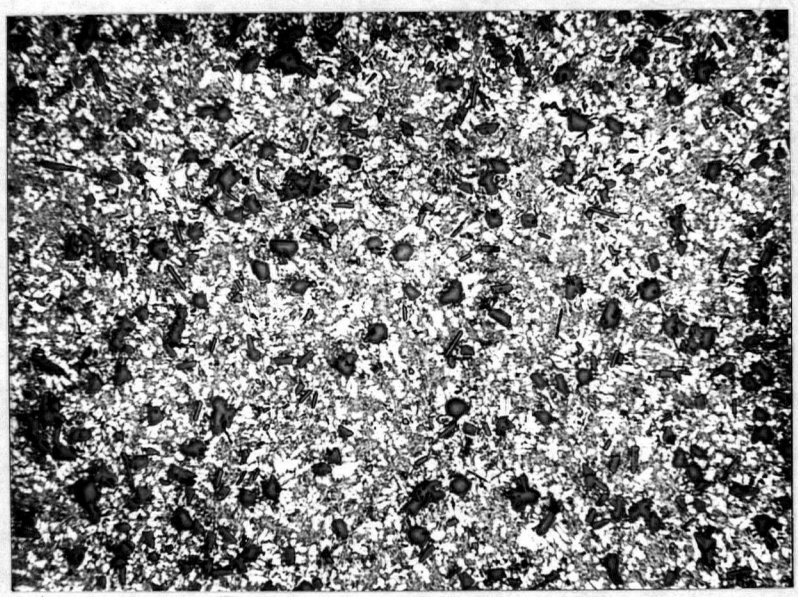

Figure 20. Alloy No. 8 refined by 0.32% P added as PCl_5. Cast 30 minutes after PCl_5 added. 0.5% HF etch. 150x

TABLE 2a.

Phosphorus Content, Primary Interparticle Spacing, and Casting Conditions for Alloys Containing Only Phosphorus.

Alloy No.	% Phosphorus	Primary Interparticle Spacing	Casting Conditions
1	0	0.079 cms.	Cast after 5 mins.
2	contaminated	—	" " "
3	0.002	0.032	" " "
4	0.007	0.031	" " "
5	0.03	0.029	" " "
6	0.12	0.025	" " "
7	0.32	0.021	" " "
8	0.32	0.015	" " 30 mins.

c. the shape of the primary silicon varies from irregular in the unrefined alloy to regular and geometric in the refined alloys (Figures 15 to 20).

d. for a constant phosphorus content the time of holding the alloy molten after adding phosphorus pentachloride has a large effect on primary interparticle spacing (Figures 19 and 20).

e. the coarseness of the eutectic increases, while the shape of the eutectic silicon remains essentially unchanged with increasing phosphorus content (Figures 21, 22 and 23). It was also observed that the coarsest eutectic in a given alloy was always closest to the primary silicon particles.

The differences in structure observed between the unrefined and refined alloys can best be explained by considering the solidification process in each case.

In a molten aluminum-20% silicon alloy it can be assumed that there will be a number of accidental foreign particles present which are solid above

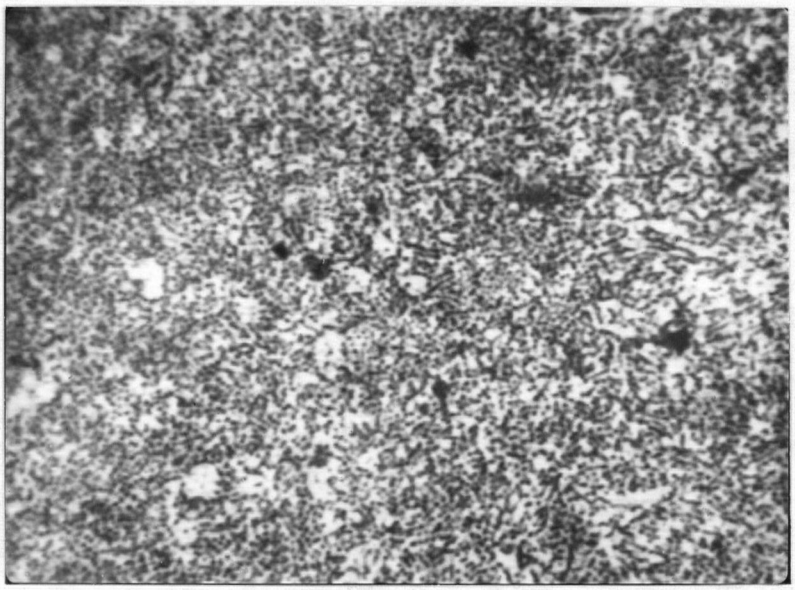

Figure 21. Finest eutectic present in unrefined alloy. (Alloy No.1). 0.5% HF etch. x 2500

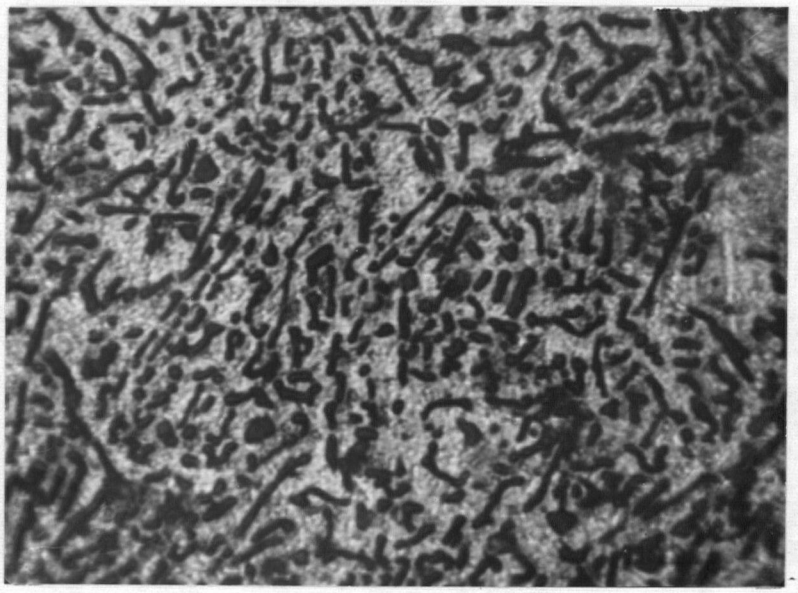

Figure 22. Finest eutectic present in PCl_5 refined alloy containing 0.12% P (Alloy No.6). 0.5% HF etch x 2500.

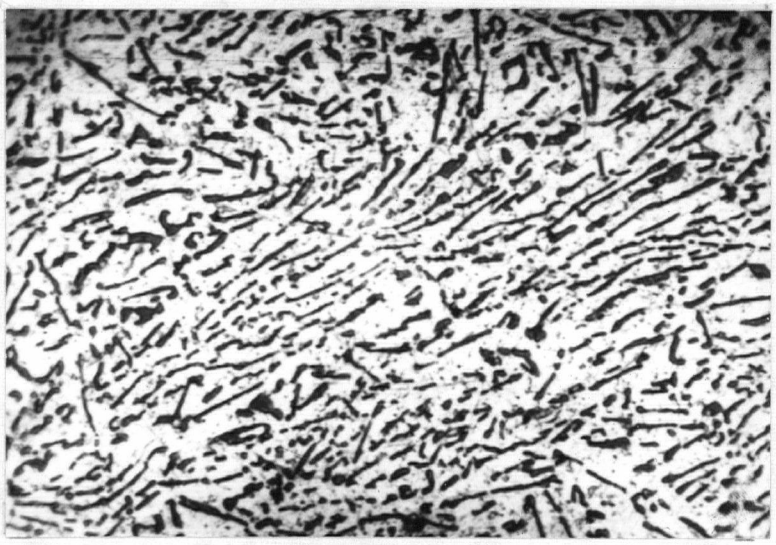

Figure 23. Finest eutectic present in PCl_5 refined alloy containing 0.32% P (Alloy No.7). 0.5% HF etch x 2500.

the liquidus temperature of the alloy. The ability of these particles to nucleate silicon heterogeneously on solidification will depend on the factors discussed in Appendix A. Some of these particles will be removed during a fluxing treatment, but some may be expected to remain or re-form, and upon cooling of the alloy these may cause heterogeneous nucleation of primary silicon.

Since an unrefined alloy may be expected to contain relatively few active heterogeneities above the liquidus temperature, only a few primary silicon particles will be nucleated on cooling. A phosphorus-refined alloy on the other hand contains aluminum phosphide particles above the liquidus, all of which will be extremely active nucleators of silicon on cooling. The number and size of the primary silicon particles will vary with the number of active nuclei present at the liquidus temperature which in the case of the artificially refined alloys may be expected to vary with the phosphorus content, at least within the range covered in the present study.

The shape of the primary silicon particles will depend upon the degree of undercooling required before nucleation of the primary silicon particles is possible. The degree of undercooling in turn will depend upon the type of heterogeneities present.

The reason for this latter dependence is that the rate of growth of a crystal in a liquid medium depends upon two factors, the specific rate of growth and the rate of transport. The specific rate of growth may be defined as the rate with which a crystal would grow if it were growing in a liquid composed entirely of its own atoms, or the rate at which atoms cross from the liquid to the solid under such conditions. The rate of transport is the actual rate with which the desired atoms are transported to the crystal faces. This will be the product of the rate of volume diffusion and a factor greater than unity to allow for any convection currents in the liquid. The rate of transport will depend upon the temperature, composition, and properties of the liquid alloy, while the specific rate of growth will depend primarily upon the crystal habit of the growing crystal and the degree of undercooling. The rate of transport will decrease with increasing undercooling and increasing viscosity of the liquid, and will also be influenced by the nature and concentration of foreign atoms present. The specific rate of growth will increase with increasing undercooling.

Therefore it may be postulated that where a certain amount of undercooling of the liquid alloy is required before any of the solid foreign particles present can act as a nuclei for the crystal precipitating, the undercooling may decrease the rate of transport and increase the specific rate of growth until they are of the same order. In this case, a zone depleted in the atoms of the crystal precipitating, will develop around the new crystal. The shape of this depleted zone will depend on the specific rates of growth

of the crystal in the various crystallographic directions. For a material which solidifies with a cubic habit the depleted zone will, in section, have the shape shown in Figure 24. Since the distance an atom must move through the depleted zone is a minimum at the corners and only slightly more at the edges of the cube, the greatest rate of growth will be from the corners of the crystal as shown in Figure 25. This will give rise to the formation of a dendritic type of crystal. If the undercooling is severe enough to decrease

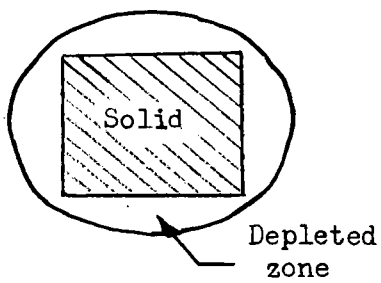

Figure 24. Section through depleted zone around a cubic crystal[14]

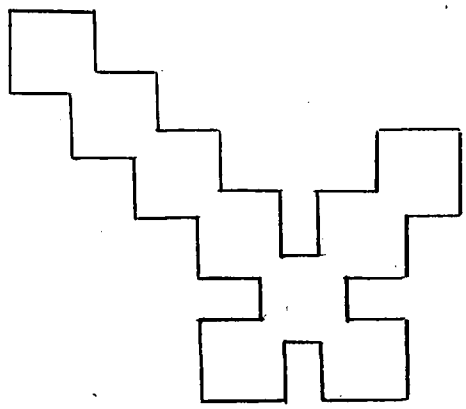

Figure 25. Dendritic type of crystal.[14]

the rate of transport even further the shape of the resulting crystal will be determined by the rate of transport alone. This will give rise to a spherical shaped crystal.

In the case of the unrefined aluminum-20% silicon alloy it can be postulated that the amount of undercooling required before any chance foreign particles present in the liquid alloy are able to act as nuclei might be enough to decrease the rate of transport and increase the specific rate of growth until they are of the same order. This would cause the primary silicon to take on a form approaching the dendritic form described above. As can be seen in Figure 15 the primary silicon particles do tend to have long dendritic-type appendages in the unrefined alloy.

However in the case of a phosphorus-refined aluminum-20% silicon alloy the aluminum phosphide particles can act as nuclei for primary silicon solidification at almost no undercooling. Therefore, since the rate of transport will be high, the limiting factor is more likely to be the specific rate of growth. Under such conditions, the primary silicon particles will tend to develop their natural crystal habit. This is evident in Figures 16 to 19.

As can be seen from Table 2a and Figures 19 and 20 the effect of the time of holding a melt after a phosphorus pentachloride addition is very significant. The reason for this time dependence is believed to be twofold. First, since the formation of aluminum phosphide requires that a chemical reaction occur between aluminum and phosphorus pentachloride the amount of aluminum phosphide formed will initially be time dependent. Second, aluminum phosphide must form in the melt by a nucleation and growth mechanism. Growth, involving time, is required to obtain phosphide particles which have radii greater than the 'critical' radius, i.e., the radius of the smallest nuclei stable in the melt, if they are to act as nuclei for the primary solidification at negligible undercooling. Agglomeration of phosphide particles would also be expected to occur with time, and this would tend to reduce the number of active nuclei available for primary solidification.

The resultant of these processes should cause an initial increase in the number of active aluminum phosphide particles present until a maximum is reached. Beyond this point agglomeration and further growth of the aluminum phosphide particles will become the dominating process and will decrease the number of effective heterogeneous nuclei. The overall time effect is indicated schematically in Figure 26. From the present work, it appears that the maximum in the curve corresponds to a substantial period of

time, at least of the order of thirty minutes. Other workers[11,12] have observed a decrease in the primary silicon dispersion with longer holding

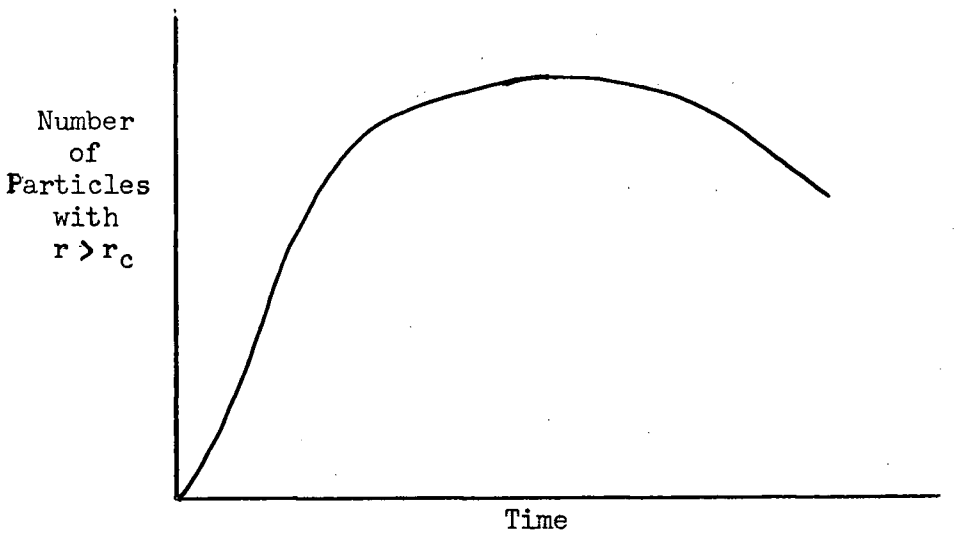

Figure 26. Number of particles with $r > r_c$ vs. time.

periods which would be expected to be a result of appreciable agglomeration of stable phosphide particles.

The increase in the coarseness of the eutectic with increasing phosphorus content is believed to be associated with the corresponding increase in the dispersion of the primary silicon.

Two mechanisms for eutectic solidification have been proposed. The first is that the nucleation and growth of one phase of the eutectic so changes the local concentration of the surrounding liquid that it becomes supersaturated with respect to the other phase. The second phase then nucleates and forms a crystal. This process continues giving first one phase and then the other. This intermittent or alternate solidification of two phases, has been rejected by Chalmers[15] for the aluminum-silicon eutectic because the aluminum is observed to form a continuous matrix around the silicon. Chalmers therefore suggests that a second mechanism, one of

simultaneous crystallization of the two phases, applies in the aluminum-silicon eutectic solidification.

The rate of advance of the solid-liquid eutectic interface depends on the balance between the rate of heat flow from the liquid to the solid through the interface, and the magnitude of the latent heat evolved during solidification. The thermal conductivities of aluminum and silicon are 0.53 and 0.20 cal/cm^2/cm/°C, respectively, while the latent heats of fusion are 94.6 cal/gr. for aluminum and 337 cal/g for silicon. These figures may not hold exactly under the conditions of eutectic solidification, but because of the large difference between them it seems obvious that the aluminum solid solution interface will advance more rapidly, as it has the lower latent heat of fusion and the higher heat conductivity. If the aluminum solid solution interface advances more rapidly than the silicon interface, and since a solid phase grows in a direction perpendicular to its surface, the aluminum solid solution can completely surround the silicon at high rates of cooling.

In the slow cooled case the silicon plates continue to grow and prevent undercooling of the liquid by acting as seed crystals on which growth can continue. In the case of rapid cooling the silicon particles are 'sealed off' from the liquid and further solidification of silicon can only occur as the result of further homogeneous nucleation which occurs at a lower temperature.

In the present work the cooling rate was high, such that a modified type of eutectic was obtained throughout in the unrefined alloys. However, in the refined alloys the matrix was found to be a mixture of modified and coarse eutectic. This indicates differences in cooling rate within the refined alloys. The regions of the alloy which incorporate primary silicon particles will cool slower than silicon-free areas because of the high latent heat of fusion

and low thermal conductivity of silicon. Therefore the liquid alloy which is most remote from primary silicon will solidify first, with some degree of undercooling, and may have a modified structure if rapid heat removal is afforded by the mould. Solidification of the remaining liquid will proceed from these original low temperature areas toward primary silicon, and the rate of eutectic solidification will be progressively slower as the primary silicon particles are approached. Thus the eutectic silicon may be expected to be appreciably coarser near the primary silicon particles, as was observed consistently in the present work.

From the above it follows that the greater the dispersion of primary silicon the more uniform will be the structure of the eutectic since there are much smaller thermal gradients existing in the alloy (Figure 19). Further, the finest eutectic structure formed in the presence of highly-dispersed primary silicon crystals may be expected to be coarser than the finest eutectic formed in the presence of coarse primary silicon (Figures 21, 22, and 23).

The possibility that phosphorus has the opposite effect to sodium on the interfacial energy relationship between solid aluminum, solid silicon, and the liquid, thereby causing a coarse normal eutectic to form even at high rates of cooling has also been considered. This has been rejected on the grounds that large variations in eutectic structure were observed within a given alloy.

2. Alloys containing phosphorus and magnesium.

In this group of alloys a constant magnesium content was maintained while the phosphorus content was varied. Magnesium was added as the pure metal and phosphorus as phosphorus pentachloride. Alloy number 1 is the control alloy and alloy number 9, which contains magnesium only, is a secondary control alloy.

It can be seen from Table 2b and Figures 15, 27, 28 and 29 that:

a. magnesium alone has a refining effect on hypereutectic silicon, 0.5% being roughly equivalent to 0.007% phosphorus (when added as phosphorus pentachloride) in terms of primary dispersion obtained.

b. magnesium and phosphorus have a marked cumulative refining effect on the hypereutectic silicon particles.

TABLE 2b.

Phosphorus Content, Primary Interparticle Spacing and Fluxing and Alloying Order for Alloys Containing Phosphorus and Magnesium.

Alloy No.	% Phosphorus	% Magnesium	Primary Interparticle Spacing	Fluxing and Alloying Order
1	0	0	0.079 cms.	
9	0	0.5	0.031	Fluxed after Mg added
10	0.12	0.5	0.020	Fluxed before Mg and PCl_5 added
11	0.20	0.5	0.029	Fluxed before PCl_5 after Mg added.

c. in the case of combined phosphorus and magnesium additions, the sequence in which the additions are made affects the degree of refinement of the primary silicon. If magnesium is added before phosphorus, there is only a minor improvement in dispersion over that observed for magnesium alone and not as great a dispersion as for the same level of phosphorus alone (Figures 29 and 27). If magnesium is added after phosphorus, a pronounced improvement in refinement over that due to either addition alone is observed.

d. the primary silicon particles are more rounded in outline in the alloys refined with phosphorus and magnesium together than

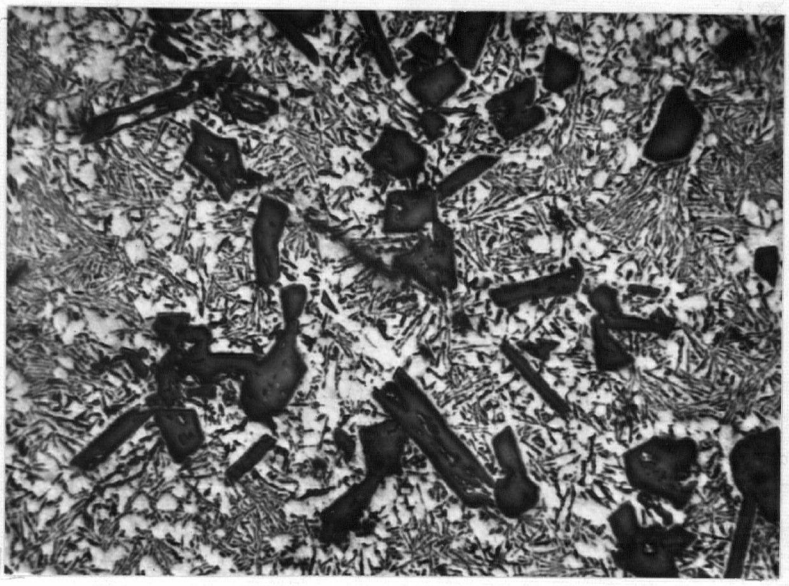

Figure 27. Alloy No. 9 containing 0.5% magnesium. 0.5% HF etch. 150x

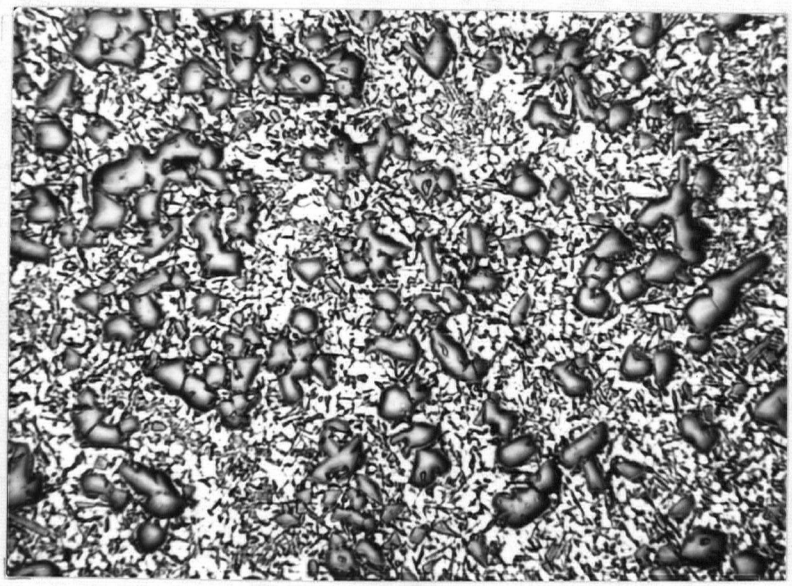

Figure 28. Alloy No. 10 containing 0.5% magnesium and 0.12% phosphorus. 0.5% HF etch 150x

Figure 29. Alloy No. 11 containing 0.5% magnesium and 0.2% phosphorus, 0.5% HF etch. 150x

in alloys refined by phosphorus alone.

e. the eutectic coarseness in these alloys increases with decreasing primary interparticle spacing.

There are three possible mechanisms whereby magnesium can cause refinement of the primary silicon. These are:

a. nucleation of primary silicon by a stable magnesium compound formed in the liquid alloy.

b. restriction of silicon crystal growth by a concentration gradient effect.

c. restriction of silicon crystal growth by the adsorption of magnesium atoms onto primary silicon.

In the case of refinement by magnesium plus phosphorus, only the latter two possibilities apply unless any magnesium compound which is formed has at least the same activity or nucleating ability as aluminum

phosphide.

A study of the magnesium compounds which might be expected to form in the melt shows that none of them has a crystal structure or lattice parameters that will permit it to compete with aluminum phosphide as a nucleator of silicon.

When magnesium was added before phosphorus pentachloride it is likely that it was partially removed by the carbon tetrachloride fluxing and partially removed by the fluxing action of the phosphorus pentachloride additions. It would probably be removed as magnesium chloride, which is a liquid at the casting temperature. It has been observed by Rosenhain, Grogan, and Schofield[29] that the magnesium content of eutectic aluminum-silicon alloys decreased when titanium tetrachloride was bubbled through the molten alloy. Thus the reason for the observed difference in the degree of refinement with the order of magnesium and phosphorus additions may be due simply to a difference in residual magnesium contents of the alloy.

This in turn suggests that the refining effect of magnesium is due to growth restriction by concentration gradients rather than by adsorption phenomena, since Northcott[2,3] found that when grain refinement could be attributed to an adsorption phenomenon the degree of refinement did not vary with solute concentration over a large range.

The belief that the refining mechanism in this case is growth restriction by concentration gradients is further supported by the typically rounded appearance of the primary silicon in Figure 27. The rounded appearance may be attributed to a decrease in the rate of transport of silicon because of concentration gradients set up by magnesium atoms.

Therefore, the marked refining effect of magnesium plus phosphorus is believed to be caused by a combination of the formation of silicon crystallites on aluminum phosphide nuclei, with almost no undercooling of the melt, plus the concentration gradients established around these crystallites by the magnesium atoms which induce nucleation to occur on further available aluminum phosphide particles not previously effective. Refining due to magnesium alone is believed to be caused by the same mechanism, but with aluminum phosphide particles being replaced by less active and less numerous heterogeneities.

The explanation offered for the mixed eutectic structure in these alloys is the same as was used previously for alloys containing phosphorus only.

3. Alloys containing phosphorus and germanium

The effect of additions of germanium to hypereutectic aluminum-silicon alloys with and without phosphorus additions has been studied. It was felt that the high solubility of germanium in solid silicon might influence the specific rate of growth of silicon as well as the rate of transport of atoms to the growing crystallites of silicon during solidification. This might be expected to lead to primary refinement by the mechanism of growth restriction. Germanium was added to these alloys as the pure metal and phosphorus as the pentachloride salt. The unrefined alloy, number 1, is again included for comparison in Table 2c.

TABLE 2c.

Phosphorus Content, Germanium Content and Primary Interparticle Spacing for Alloys Containing Phosphorus and Germanium.

Alloy Number	% Phosphorus	% Germanium	Primary Interparticle Spacing cms.
1	-	-	0.079
12	0.09	0.1	0.025
13	0.009	0.5	0.042
14	0.009	1.0	0.031

The only refinement observed in these alloys appears to be that due to phosphorus. This may be seen by comparing the primary interparticle spacing of alloy 14 with 4 and alloy 12 with 6. Also the shape of the primary silicon particles is the same as was observed in alloys containing the same level of phosphorus only. The lack of refinement in alloy 13 cannot be satisfactorily explained. If germanium, in the concentrations used, has had any growth restriction effect on silicon it has not been manifested in measurable primary refinement.

Thus it appears that the introduction of concentration gradients within the primary crystallites does not have a similar effect to concentration gradients within the liquid surrounding primary silicon such as were obtained through additions of magnesium..

4. Alloys containing phosphorus and copper.

Phosphorus additions to these alloys were made in the form of a copper-phosphorus alloy (85% copper and 15% phosphorus). Additional copper, as required to bring the total to 1.77%, was added as elemental copper, except for alloy 20 which contained only 0.97% copper. Alloys 1 and 15 are control alloys for this group.

It can be seen from Table 2d and Figures 29 and 30 that

a. copper alone has a refining effect on hypereutectic silicon, 1.77% copper being equivalent to 0.007% phosphorus added as phosphorus pentachloride, or 0.5% magnesium added as elemental magnesium.

b. the maximum refining effect of phosphorus in the presence of copper when added by means of a copper-phosphorus alloy,

TABLE 2d.

Phosphorus Content, Copper Content and Primary Interparticle Spacing for Alloys Containing Phosphorus and Copper.

Alloy Number	% Phosphorus	% Copper	Primary Interparticle Spacing cms.
1	0	0	0.079
15	0.	1.77	0.030
16	0.005	1.77	0.026
17	0.01	1.77	0.027
18	0.05	1.77	0.025
19	0.20	1.77	0.029
20	0.01	0.97	0.027

occurs at 0.005% phosphorus and then holds essentially constant at higher levels up to 0.20%. There is an indication that a slight loss of primary refinement resulted from the addition of more than 0.1% phosphorus in these alloys.

c. the shape of primary silicon particles is irregular in the copper and copper-phosphorus refined alloys.

d. a relatively small variation in the copper content of the alloy has no noticeable effect on the refinement of the primary silicon (alloys 17 and 20).

e. the eutectic in the unrefined alloy was predominately modified with a small amount of coarse normal eutectic. The eutectic became coarser with the addition of phosphorus and copper until higher phosphorus contents (0.2%) were reached at which point the eutectic again appeared to become more refined.

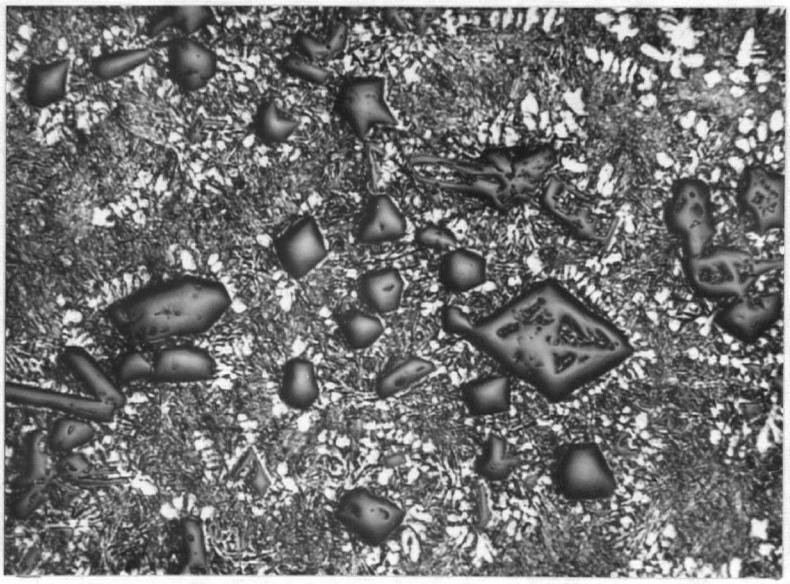

Figure 30. Alloy No. 15 containing 1.77% copper. 0.5% HF etch. 150x

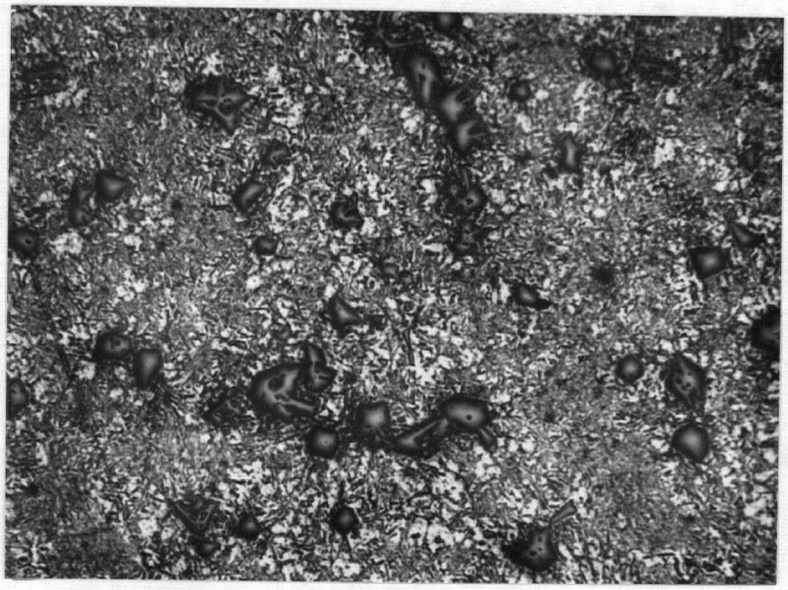

Figure 31. Alloy No. 18 containing 1.77% copper and 0.05% phosphorus added as phosphorus-copper. 0.5% HF etch. 150x

The rather limited refining effect of copper plus the irregular shape of the primary silicon in these alloys indicates that growth restriction by concentration gradients is an active refining mechanism in these alloys.

The variation in the coarseness of the eutectic follows the variation in the refinement of primary silicon according to the theory advanced previously for the case of phosphorus-pentachloride refined alloys.

The degree of comminution of additions to aluminum-silicon alloys has been found by other workers to have a major effect on the refinement obtained for a constant level of refining addition. Kessler and Winterstein,[30] who actually ground their refining additions to different particle sizes, have studied this variable extensively. In the previously described experiments with phosphorus pentachloride fluxing it would be expected that an excellent dispersion of phosphorus in the melt would be effected due to the volatility of the additions.

This dependence of refinement on the degree of dissemination of the phosphorus addition is explained by the fact that the greater the dispersion of the phosphorus the larger the number of aluminum phosphide particles that will be formed and the greater the primary refinement on solidification.

In the present work, phosphorus copper additions were made in the form of spherical granules ranging in size from 1 to 5 mms. in diameter. In the case of low phosphorus alloys several small granules of phosphorus copper were used, while for the larger additions, a few larger granules were used.

This is believed to account for lack of increased primary refinement which would normally have been expected to accompany an increase in total

phosphorus addition as phosphorus copper. It also may account for the observation that the best primary refinement obtained with phosphorus copper was not as intense as that obtained by phosphorus pentachloride fluxing.

B. Mechanical Tests

1. Tensile tests

The results of tensile tests were not reproducible because of gas porosity in the castings. As a result, no conclusions can be made as to the specific effect of structural refinement on the yield point and ultimate strength directly, but must be inferred from hardness results.

2. Hardness tests

The variation in hardness with refinement was recorded for all of the alloys prepared and the following trends appeared (see Table 2, Appendix D).

a. the presence of phosphorus alone reduces the hardness of the alloys significantly below the level for the unrefined alloy.

b. the presence of magnesium with or without phosphorus increases the hardness of the alloy significantly above that for the unrefined alloy.

c. the presence of copper did not affect the hardness of the unrefined alloy appreciably.

Three factors are interacting to give the observed variation in hardness. These are the variation in primary refinement, the variation in the eutectic structure, and the matrix-strengthening effect of additions which enter into solid solution in aluminum.

In the alloys refined with phosphorus only there is an extreme coarsening of the eutectic even with small phosphorus additions. This, in spite of the accompanying primary refinement, will greatly increase the mean free path through the aluminum solid solution and will therefore decrease the overall hardness of the alloy. Increasing the phosphorus content beyond a very low value did not result in a further major coarsening of the eutectic structure; therefore, it would not be expected that hardness of the alloy should drop significantly lower with increasing phosphorus content, at least in the range of compositions investigated.

In the case of magnesium-refined alloys there is an appreciable matrix hardening due to the solid solution of magnesium in aluminum as shown by comparing alloys 1 and 9. The consistancy of hardness through the three alloys 9, 10 and 11 is probably due to the combined effects of a variation in primary dispersion, the accompanying variation in eutectic coarseness, and the suspected variation in magnesium content mentioned previously.

The reason that the alloys which were refined with copper had approximately the same hardness as the unrefined alloy is believed to be due to the compensating effects of eutectic coarsening (through increased primary refinement) and the solid solution hardening effect of copper in aluminum. This is borne out by comparing alloys 20 and 17.

As is obvious from the preceding discussion the increase in hardness which was expected to accompany an increasing primary dispersion was not realised, because of the coarsening of the eutectic which paralleled the increased primary dispersion.

The only conclusions which can be made as to the variation in tensile strength and yield point of these alloys must be drawn from the

hardness results. Since tensile strength and yield point may be assumed to vary in the same manner as hardness, the preceding observations should also apply qualitatively to tensile strength and yield point. This correlation has been observed by other workers.[14,17]

IV. CONCLUSIONS

Primary refinement in hypereutectic aluminum-silicon alloys has been found to be accompanied by a substantial overall coarsening of the eutectic structure, with a resultant decrease in hardness of the alloys. This is in contradiction to the common belief that refinement of primary silicon is responsible for a major improvement in mechanical properties.

The eutectic coarsening is believed to result from a reduction in temperature gradients in the liquid during solidification, which in turn results from a greater dispersion of primary silicon.

It has been shown that the refining mechanism for both magnesium and copper additions is growth restriction due to concentration gradients. The extra refining effect of phosphorus plus magnesium and phosphorus plus copper is believed to be due to the nucleation of silicon on new aluminum phosphide nuclei caused by concentration gradients set up around the growing silicon crystallites.

The effect of the time the alloy is held molten after phosphorus is added as the pentachloride is believed to be due to an increase with time in the number of active aluminum phosphide particles present in the melt. This is because of the time dependance of the nucleation and growth of the aluminum phosphide particles.

The variation in shape of the primary silicon between the unrefined and refined alloys is due to variations in the rate of atom transport in the liquid, caused by variations in the degree of primary undercooling and by concentration gradients.

The variation in hardness of the alloys tested was found to be due to three factors. These were coarseness of the eutectic, degree of dispersion of primary silicon, and the solid solution of refining additions in the aluminum.

APPENDIX A

Ability of Foreign Particles to Cause Heterogeneous Nucleation.[1]

Only certain types of foreign particles will reduce the free energy required to create the new interfaces when a crystallite is formed, and it is only to these nuclei that Figure 2 refers; other particles may be ineffective. The properties which enable a foreign particle to act as a nucleus may be derived as follows:

$$\Delta G' = \Delta G_1' + \Delta G_2' \qquad (1)$$

ΔG_1 = free energy change due to phase change

$$= K_1 \text{ x volume of solid crystallite} \qquad (2)$$

where K_1 corresponds to a degree of undercooling, ΔT_1, and is zero when $\Delta T = 0$

ΔG_2 = free energy change due to the formation of new interfaces

$$= \Sigma(K_{AB} \text{ x area of interface A/B}) \qquad (3)$$

where K_{AB} is the free-energy content per unit area of the interface A/B. In the following, where equation (3) is used,

$K_{SL} \equiv$ solid metal-liquid metal interface

$K_{SP} \equiv$ solid metal-foreign particle interface

$K_{LP} \equiv$ liquid metal-foreign particle interface.

The interfacial free-energy contents may be treated as forces acting in the respective interfaces (i.e. 'surface tensions'). Ideally the relation between K_{SL}, K_{LP}, and K_{SP} governs the angles of contact of interfaces, as in Figure a, such that:

$$K_{LP} = K_{SP} + K_{SL} \cos \theta \qquad (4)$$

This idealized relationship is used below to investigate the effects of the properties of the interfaces upon crystallite formation; in practice this assumption must be qualified because the shape of the

APPENDIX A (cont'd.)

crystallite and the angles of contact will also be controlled by crystal forces and by the variation of rates of growth with lattice direction.

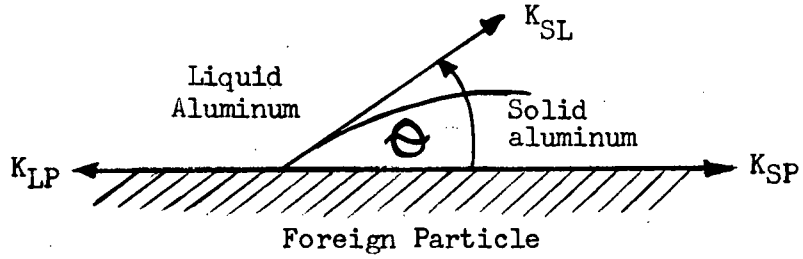

Figure a. Relation between interfacial free-energy contents and angles of contact.

Three types of crystallite formation may occur, theoretically, as in (a), (b), and (c) below.

Type (a). $$K_{SP} \gg K_{SL} + K_{LP} \qquad (5)$$

The angle of contact θ is 180°C, and new crystallites are therefore formed as spheres (minimum surface area to volume ratio), either touching the foreign particle or away from it, and the free energy of the surface of the crystallites is not affected by the presence of the particles; nucleation therefore occurs as in a melt free from such inclusions. Re-arranging equation (5)

$$K_{SL} + K_{LP} - K_{SP} \ll 0$$

$K_{SL} + K_{LP} - K_{SP}$ is the work per unit area required to part a crystallite of solid aluminium from the surface of a foreign particle, when immersed in liquid aluminium, and is known as the 'work of adhesion'. Hence, when the work of adhesion is less than zero (i.e. adhesion is unstable), crystallite formation occurs as in a melt free from foreign particles.

APPENDIX A (cont'd.)

Type (b) $$K_{LP} > K_{SP} + K_{SL} \qquad (6)$$

$$\Delta G = \Delta G_2 + \Delta G_1$$

$$= (K_{SP} + K_{SL} - K_{LP}) \text{ x area of film} - K_1 \text{ x volume of film} \qquad (7)$$

< 0 at all stages in the growth of the crystallite, since both terms are negative.

The smallest of these crystallites is therefore stable (even slightly above the true melting point, when K_1 is negative).

Since $K_{LP} > K_{SL} + K_{SP}$ (6)

$$K_{SL} + K_{LP} - K_{SP} > 2\,K_{SL} \qquad (8)$$

The quantity of $2\,K_{SL}$ is the work of cohesion of two surfaces of solid metal in liquid; thus when the work of adhesion of solid metal to a foreign particle is greater than the work of cohesion of solid metal crystallite formation occurs very readily, the work of formation being negative at all stages, at a temperature at or below the melting point.

Type (c)

Between types (a) and (b), a continuous range of crystallite formation is possible, such that:

$$K_{LP} < K_{SL} + K_{SP} \quad \text{and} \quad K_{SP} < K_{SL} + K_{LP} \qquad (9) \text{ and } (10)$$

and θ lies between 0 and 180°, as, for example, in Figure a. It may be assumed that, at least initially, the crystallite is approximately in the shape of a spherical cap, the base angles being fixed by the relation above in equation (4). Then

$$\Delta G = \Delta G_2 + \Delta G_1 \qquad (1)$$

APPENDIX A (cont'd.)

$$\Delta G = \left[K_{SL} \cdot 2\pi r^2 (1 - \cos\theta)^2 + (K_{SP} - K_{LP})\pi r^2 \sin^2\theta\right] - \left[K_1 \frac{\pi r^3}{3}(1 - \cos\theta)^2(2 + \cos\theta)\right]$$

where r is the radius of the spherical cap

ΔG is a maximum when $\frac{\partial \Delta G}{\partial r} = 0$,

i.e., when $r = \frac{2\left[2 K_{SL} + (K_{SP} - K_{LP})(1 + \cos\theta)\right]}{K_1(1 - \cos\theta)(2 + \cos\theta)}$

and $\Delta G_{max} = (K_{SL} + K_{SP} - K_{LP})^2 (2 K_{SL} + K_{LP} - K_{SP}) \frac{4\pi}{3K_1^2}$ (11)

This expression decreases continuously from $\frac{16\pi}{3K_1^2} K_{SL}$, when $K_{LP} + K_{SL} - K_{SP} = 0$, (i.e. Type (a)), to zero when $K_{LP} + K_{SL} - K_{SP} = 2K_{SL}$ (i.e. Type (b)). (Outside these limits, the values of θ given by equation (11) are unreal, crystallites forming as in Type (a) or (b) above).

The values of ΔG are plotted in Figure b against W_A, the work of adhesion of solid metal to foreign particle, over the three ranges of crystallite formation.

To summarize, crystallite formation occurs more readily with a corresponding reduction in undercooling, in the presence of foreign nuclei to which the work of adhesion (of solid metal) is greater than zero; when the work of adhesion is equal to or greater than the work of cohesion of solid metal (as in Type (b) above), crystallites are more stable than the liquid phase at all particle sizes and undercooling should be impossible.

APPENDIX A (cont'd.)

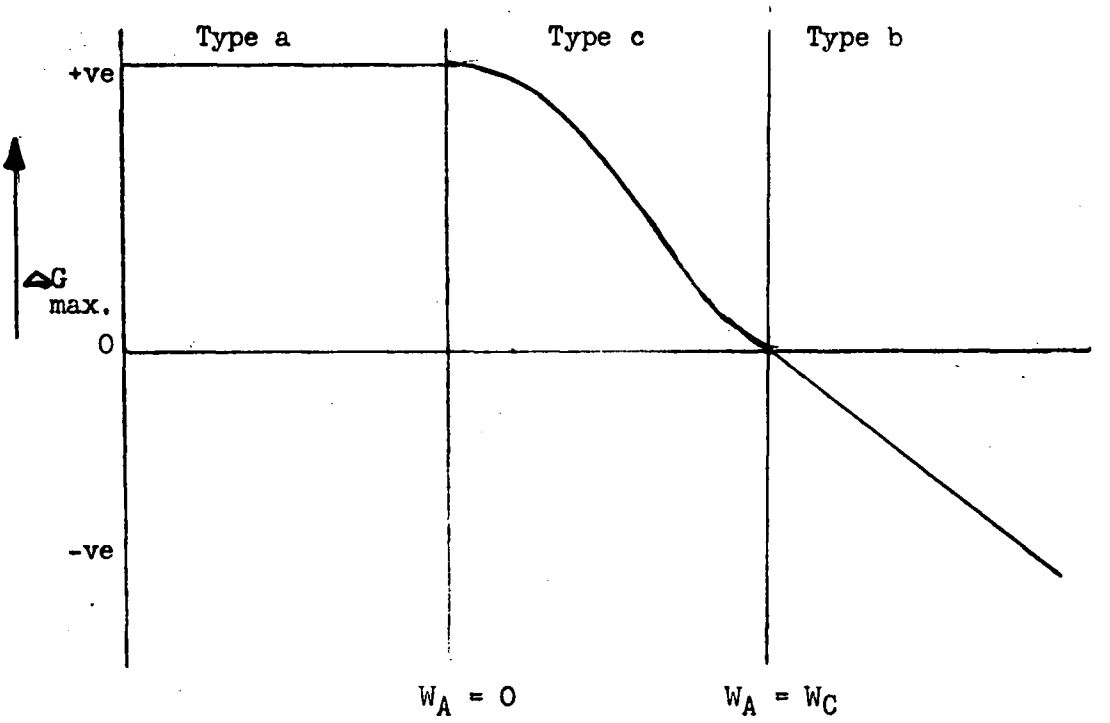

Figure b. ——— W_A ⟶
KEY

Type (a) - crystallite formation and undercooling not affected by presence of particles.

Type (b) - crystallites form as films on foreign particles with no undercooling.

Type (c) - crystallites form more readily on foreign particles with diminished undercooling.

W_A = work of adhesion of metal (solid) to surface of foreign particle.

W_C = work of cohesion of solid metal.

APPENDIX B

Analysis of Alloying Materials.

TABLE 3

Analysis of Aluminum
Supplied by the Aluminum Company of Canada Ltd.

Element	Concentration
Aluminum	99.99%
Iron	0.002
Magnesium	0.002
Copper	0.001
Silicon	<0.001

TABLE 4.

Analysis of Silicon
Supplied by the Electro Metallurgical Company

Element	Concentration
Silicon	99.80%
Iron	0.017
Aluminum	0.022
Carbon	0.04
Calcium	0.005
Magnesium	0.003
Phosphorus	0.006
O_2	0.05
H_2	0.002
N_2	0.01

APPENDIX B (cont'd.)

TABLE 5

Analysis of Copper

Element	Concentration
Copper	99.9%
Insolubles	0.002
Manganese	0.001
Phosphorus	0.001

TABLE 6

Analysis of Phosphorus Pentachloride

Element	Concentration
Residue after ignition	0.01%
Sulphate	0.005
Heavy metals	0.001
Iron	0.001

TABLE 7

Partial Analysis of Phosphorus Copper, Magnesium, and Germanium.

Element	Concentration	Element	Concentration	Element	Concentration
Phosphorus plus copper	99.75% min.	Magnesium	99.8%	Germanium	99.0%
Phosphorus	14.5 - 15.5%	Full analysis not available.		Full analysis not available.	
Full analysis not available					

APPENDIX C

Estimate of Variation in f Due to Variation in Silicon Content of Alloy.

Estimate of the variation in f to be expected from a variation in the silicon content of an aluminum - 20% silicon alloy.

$$f = \frac{\text{Volume of primary silicon}}{\text{Volume of matrix (eutectic)}}$$

For 19.0% silicon

$$f = \frac{19 - 11.6}{2.42} \times \frac{2.66}{100 - 19} = 0.101$$

For 21% silicon

$$f = \frac{21 - 11.6}{2.42} \times \frac{2.66}{100 - 21} = 0.131$$

Value previously calculated for 20% silicon = 0.116

Therefore variation in f due to ±1% variation in silicon is ±0.015 or ±12.9%.

APPENDIX D

TABLE 2

Composition, Primary Interparticle Spacing, and Hardness of Alloys Studied

Alloy No.	COMPOSITION*				Primary inter-particle spacing** cms.	HARDNESS	
	% P	% Cu	% Mg	% Ge		R_f	KNOOP
1	0	-	-	-	0.079	82.7 ± 0.7	80.4 ± 3.5
2	Contaminated		-	-			
3	0.002	-	-	-	0.032	74.8 ± 1.5	74.2 ± 2.6
4	0.007	-	-	-	0.031	76.1 ± 0.6	
5	0.03	-	-	-	0.029	73.6 ± 1.4	72.9 ± 2.5
6	0.12	-	-	-	0.025	74.8 ± 4.1	
7	0.32	-	-	-	0.021	75.0 ± 1.5	
8	0.32	-	-	"	0.015	76.4 ± 1.0	
9	-	-	0.5	"	0.031	87.6 ± 0.6	101.0 ± 3.2
10	0.12	-	0.5	"	0.020	86.7 ± 0.7	101.1 ± 1.2
11	0.20	-	0.5	"	0.029	85.8 ± 0.7	93.7 ± 2.0
12	0.09	-	-	0.1	0.025	78.8 ± 0.6	
13	0.009	-	-	0.5	0.042	78.7 ± 0.9	
14	0.009	-	-	1.0	0.031	76.5 ± 0.8	
15	0	1.77	"	-	0.030	80.9 ± 0.9	
16	0.005	1.77	"	-	0.026	84.8 ± 0.9	
17	0.01	1.77	"	-	0.027	84.6 ± 0.7	
18	0.05	1.77	"	-	0.025	82.9 ± 0.8	
19	0.20	1.77	"	-	0.029	83.4 ± 1.0	
20	0.01	0.97	"	-	0.027	79.3 ± 0.9	

* By addition (assuming 100% recovery)

** These values of primary interparticle spacing have a variation of approximately ±0.002 as based on several calculations.

BIBLIOGRAPHY

1. Cibula, A., J. Inst. Metals, 76, 4, p.321, December 1949.
2. Northcott, L., J. Inst. Metals, 65, p.173, 1939.
3. Northcott, L., J. Inst. Metals, 62, p.101, 1938.
4. Smithells, C.J., Discussion, J. Inst. Metals, 62, p.122, 1938.
5. Mehl, R.F., Jetter, L.K., "Symposium on Age-Hardening of Metals," A.S.M., p.342, 1940.
6. Turnbull, D., J. App. Physics, 20, p.817, 1949.
7. Turnbull, D., Trans. A.I.M.E., 188, p.1144, 1950.
8. Mitsche, R., Carnegie Schol. Mem. Iron Steel Inst., 23, p.65, 1934, or 25, p.41, 1936.
9. Latin, A., J. Inst. Metals, 66, p.177, 1940.
10. Cibula, A., J. Inst. Metals, 80, p. 1, 1951-52.
11. Onitsch-Modl, E., "Proceedings of the First World Metallurgical Congress", A.S.M., p.325.
12. Lund, J.A., Unpublished thesis, University of Birmingham, 1953.
13. Wyckoff, "Crystal Structures", V. 1, Interscience.
14. Mascré, M.C., Fonderie, 91, p.3556, 1953.
15. Chalmers, B., J. Inst. Metals, 77, p.79, 1950.
16. Sorby, H.C., J. Iron and Steel Inst., 1, p.255, 1887.
17. Greene, O.V., Trans. Am.Soc. for Steel Treating, 16, p.57, 1929.
18. Gensamer, M., Pearsall, E., and Smith, G.V., Trans. A.S.M., 28, p.380, 1940.
19. Gensamer, M., Pearsall, E., Pellini, W.S., and Low, J.R. Jr., Trans. A.S.M., 30, p. 983, 1942.
20. Shaw, R.B., Shepard, L.A., Starr, C.D., and Dorn, J.E., Trans. A.S.M., 45, p.249, 1953.

21. Roberts, C.S., Carruthers, R.C., and Averbach, B.L., Trans. A.S.M. 44, p.1150, 1952.

22. Mott, N.F., "Imperfections in Nearly Perfect Crystals", edited by Schockley et al, John Wiley and Sons Inc., New York, p.173, 1952.

23. Orowan, E., "Symposium on Internal Stresses in Metals and Alloys", Inst. Metals, London, p.451, 1948.

24. Fisher, J.C., Hart, E.W., and Pry, R.H., Acta Met. 1, p.336, 1953.

25. Hart, E.W., "Relation of Properties to Microstructure", A.S.M., p.95, 1954.

26. Metals Handbook, A.S.M., 1948 Ed., p.1166.

27. Handbook of Chemistry and Physics, Chem. Rubber Publ. Co., 37 Ed., p.1961, 1955-56.

28. Metals Handbook, A.S.M., 1948 Ed., p. 805.

29. Rosenhain, W., Grogan, J.D., and Schofield, T.H., J. Inst. Metals, 44, p. 305, 1930.

30. Kessler, H., and Winterstein, H., Z. Metallkunde, 47, p.97, 1956.